Check for updates

The Contribution of Wind-Generated Waves to Coastal Sea-Level Changes

Guillaume Dodet[1] · Angélique Melet[2] · Fabrice Ardhuin[1] · Xavier Bertin[3] · Déborah Idier[4] · Rafael Almar[5]

Abstract

Surface gravity waves generated by winds are ubiquitous on our oceans and play a primordial role in the dynamics of the ocean–land–atmosphere interfaces. In particular, wind-generated waves cause fluctuations of the sea level at the coast over timescales from a few seconds (individual wave runup) to a few hours (wave-induced setup). These wave-induced processes are of major importance for coastal management as they add up to tides and atmospheric surges during storm events and enhance coastal flooding and erosion. Changes in the atmospheric circulation associated with natural climate cycles or caused by increasing greenhouse gas emissions affect the wave conditions worldwide, which may drive significant changes in the wave-induced coastal hydrodynamics. Since sea-level rise represents a major challenge for sustainable coastal management, particularly in low-lying coastal areas and/or along densely urbanized coastlines, understanding the contribution of wind-generated waves to the long-term budget of coastal sea-level changes is therefore of major importance. In this review, we describe the physical processes by which sea states may affect coastal sea level at several timescales, we present the methods currently used to estimate the wave contribution to coastal sea-level changes, we describe past and future wave climate variability, we discuss the contribution of wave to coastal sea-level changes, and we discuss the limitations and perspectives of this research field.

Keywords Wind waves · Sea level · Coastal zone · Climate change

✉ Guillaume Dodet
guillaume.dodet@ifremer.fr

1 UMR 6253 LOPS, CNRS-Ifremer-IRD-Univiversity of Brest Brest, ZI Pointe du Diable, CS10070, 29280 Plouzané, France

2 Mercator Ocean, 8-10 rue Hermès, 31520 Ramonville Saint Agne, France

3 UMR 7266 LIENSs, CNRS - La Rochelle University, 2 rue Olympe de Gouges, 17000 La Rochelle, France

4 BRGM, 3 avenue Guillemin, 45060 Orléans Cédex, France

5 UMR 5566 LEGOS, 18 avenue Edouard Belin, 31401 Toulouse Cédex 9, France

1 Introduction

Waves often play a significant role in high sea levels and inundations at the coast, whether associated with a local wind storm or with swells from a remote storm (Hoeke et al. 2013; Ford et al. 2018). This wave activity has a strong regional and interannual variability (Bromirski et al. 2005), and long-term trends in offshore significant wave height (H_s) exhibit strong regional variations, with possible trends of a few centimeters per year for the 90th percentile of offshore H_s (Wang and Swail 2001). The wave-driven contribution to the total water level generally varies with shoreline morphology and sea-state properties and can be a fraction of the offshore H_s that ranges from 10 to 200% (e.g., Stockdon et al. 2006; Poate et al. 2016). As a result, wave-driven contributions to the water level can contribute substantially to trends in coastal sea level (Melet et al. 2018).

The contribution of wave to coastal sea level adds to *ocean dynamic sea-level rise* (Gregory et al. 2019) and, where wave height or wave periods increase, enhances the threat to coastal zones (Cazenave and Cozannet 2014), or mitigates the threat where heights or periods decrease. First, because a higher sea level increases the frequency and amplitude of coastal hazards, such as flooding and erosion, but also because the social and economic stakes of the coasts have never been so valuable and fragile at the same time. Indeed, the increase in population density in coastal regions during the industrial period has fostered the urbanization of many coastlines of the world, enhancing their socioeconomic importance but also weakening their resilient capacity (Neumann et al. 2015). Therefore, densely populated and/or highly urbanized coastlines now require a detailed understanding of coastal sea-level changes, with possible costly adaptation strategy and accurate early warning systems in order to maintain economic activities and population safety.

Since the early 1990s, satellite altimetry has provided a comprehensive view of the global distribution of sea-level changes (Cazenave et al. 2018). However, these results concern the open ocean and, presently, cannot be easily extrapolated to the coastal regions. Indeed, coasts represent an important source of noise in radar altimetry, which prevents an accurate estimation of sea level closer than about 20 km from the coast (Cipollini et al. 2017). In addition, the coastal shelf and more particularly the narrow wave-breaking zone (with width of the order 10^1–10^4 m, Wright and Short 1984) is a very dynamic region that exhibits rapid changes in sea level and currents, as a result of the complex interactions between the waves and the sea floor (Munk and Traylor 1947). Indeed, wind-generated waves accumulate and transport momentum across ocean basins and release it to the water column when they break in the shallow surf zone. The rapid decrease in momentum flux is compensated by a tilting of the water surface between the breakpoint and the waterline (Longuet-Higgins and Stewart 1964), which can raise the time-averaged sea level at the waterline by up to 1 m (Pedreros et al. 2018; Guérin et al. 2018; Dodet et al. 2018). This effect, called the wave setup, is modulated by long waves with periods of the order of 1 min that travel at the speed of the wave groups and rapidly grow (from centimeters to decimeters) in the surf zone. These waves are called infragravity (IG) waves. Finally, the wave runup, which is the highest waterline elevation reached by individual waves, integrates both the setup and infragravity waves plus a short-wave component, and represents an important contributor of the total water level. Since the wave runup is directly responsible for wave overtopping, it is crucial to take it into account for the design of coastal defences. The wave setup, wave runup and

infragravity waves are all directly controlled by incident wave conditions and nearshore bathymetry.

Similarly to the atmospheric circulation, the average wave fields present coherent patterns at the basin scale that can be described with statistical parameters. The wave climate integrates the effect of both distant and local wind conditions, which makes the interpretation of observed variabilities particularly challenging. Thanks to long-term wave buoy records, spectral wave models and satellite-based wave observations, the different modes of variability of the wave climate have been well investigated. The strong interannual variability of H_s at high latitudes and its link with climate modes such as the North Atlantic Oscillation (NAO), the Pacific Decadal Oscillation (PDO) or the Southern Annular Mode (SAM) has been evidenced in several studies (e.g., Dodet et al. 2010; Hemer et al. 2018; Bromirski et al. 2013). Similar findings were obtained for extreme wave heights based on wave buoy and satellite observations (Menéndez et al. 2008; Izaguirre et al. 2011). Analysis of satellite-based wave observations over the period 1985–2008 highlighted the existence of significant trends in H_s in several regions of the world, more pronounced for the 90th and 99th percentiles of H_s (Young et al. 2011). However, given the relatively short time coverage of this data set, it is likely that the observed trend values are mostly influenced by decadal climate oscillations. Bertin et al. (2013) analyzed the outputs of a 109-year numerical wave hindcasts for the North Atlantic and found significant trends in H_s in the North-East Atlantic, in the absence of any trends in NAO over the same period. While these long-term trends could be the result of external climate variability, the time consistency of the wind field reanalysis that feed wave hindcasts remains a major issue to be solved for gaining confidence in such results (e.g., Stopa et al. 2019). Nevertheless, given the significant contribution of wave-induced processes to coastal sea level, changes in the wave conditions over decadal or longer timescales will likely contribute to coastal sea-level changes and need to be further investigated.

The objective of this review paper is to discuss the current state of knowledge on wind-generated wave contributions to coastal sea-level changes, how these contributions are observed and modelled, and to identify future research needs in that regard. In the following section (Sect. 2), we describe the main physical processes through which wind-generated waves can affect coastal sea level. In Sect. 3, we introduce the methods used to characterize offshore significant wave conditions and we present our current understanding on past and future wave conditions, coastal sea level and wave conditions. In Sect. 4, we present the method used to estimate nearshore parameters required to investigate coastal sea level and we discuss the impact of waves on coastal sea level. Finally, in Sect. 5, we present the current limitations of our understanding of the wave impact on coastal sea level and we mention several perspectives that could improve our understanding in the near future.

2 Physical Processes

Wave-induced processes control the nearshore hydrodynamics of exposed coastline and cause fluctuations of the coastal sea level over a wide range of timescales. Three main processes are identified and correspond to distinct, yet overlapping, spatial and temporal scales. These processes and their associated scales are depicted in Fig. 1. First, infragravity waves (Fig. 1a, d), which travel out of phase with the wave groups they are bound to, have typical periods of ~ 1 min and wavelength of ~ 10 km. Second, the wave

HOW DO WIND GENERATED WAVES IMPACT COASTAL SEA LEVEL ?
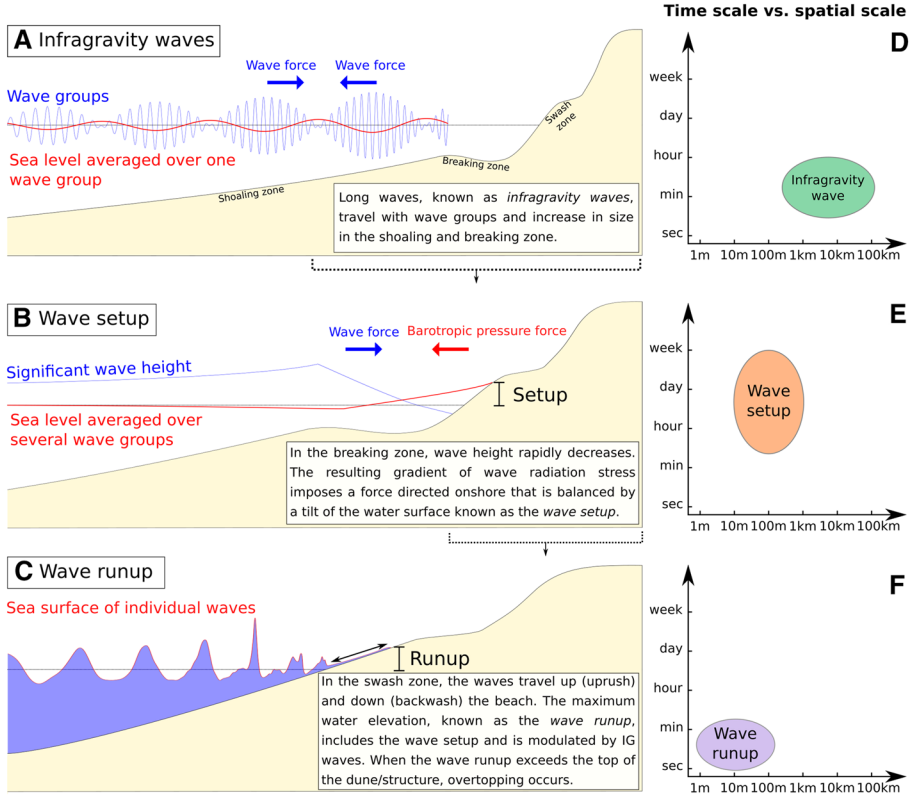
Fig. 1 Schematic description of wave-induced processes impacting coastal sea level and their associated temporal and spatial scales for **a–d** infragravity waves; **b–e** wave setup; and **c–f** wave runup. The horizontal dotted black line represents the still water level, which includes the mean sea level, the astronomical tide and the atmospheric surge components

setup (Fig. 1b, e), which develops in the surf zone, may extend from a dozen of meters in steep environments to several kilometers in low-sloping environments during stormy conditions. Since the magnitude of the wave setup is mostly controlled by the offshore significant wave height, period and spectrum shape (Guza and Feddersen 2012), its magnitude varies with local wind sea and swell conditions, from a few hours to several days. Third, the wave runup (Fig. 1c, f), which corresponds to the fluctuations of the highest instantaneous water level across the swash zone, extends from a few meters in reflective environments to a hundred meters in dissipative environments. Its timescale is controlled by the relative contribution of incident (periods of ~ 10 s) and infragravity (periods of ~ 1 min) wave energy that reach the shoreline after the incident waves have broken. These three processes all contribute to the total coastal sea level, which is here defined as the sum of the mean sea level (e.g., averaged over 1 year), the astronomical tide, the atmospheric surge (inverse barometer effect and wind-induced surge) and the wave runup. The wave runup is composed of a steady component, the wave setup, and a fluctuating component, the swash, itself composed of a high-frequency (incident waves)

component and a low-frequency (infragravity waves) component. The following paragraphs present these processes in more detail.

2.1 Wave Setup

Wave setup corresponds to the increase in mean water level along the shoreline associated with the dissipation of wind-generated waves in the nearshore and was first reported by Saville (1961). It is usually measured relative to the still water level, defined here as the mean sea level outside the surf zone, including the astronomical tide and the atmospheric surge. Wave setup was investigated based on field observations for several decades (e.g., Guza and Thornton 1981; Holman and Sallenger 1985; Raubenheimer et al. 2001; Apotsos et al. 2007; Nicolae-Lerma et al. 2017; Guérin et al. 2018). Wave setup can exceed 1 m under storm waves (Pedreros et al. 2018; Guérin et al. 2018; Dodet et al. 2018) and can therefore have a relevant contribution in storm surges. As a rough guideline, wave setup along the shoreline of sandy beaches represents about 10 to 20% of the significant wave height at the breaking point. Along the coasts bordered by narrow continental shelves or at volcanic islands, wave setup can even represent the largest contribution of storms surges (e.g., Kennedy et al. 2012; Bertin et al. 2017; Pedreros et al. 2018). Several studies also showed that the setup driven by wave breaking over the ebb deltas of shallow inlets (Malhadas et al. 2009; Dodet et al. 2013) and large estuaries (Bertin et al. 2015; Fortunato et al. 2017; Bertin et al. 2017) could propagate outside surf zones and raise the water level at the scale of the whole lagoon/estuary. The tilting of the free surface elevation resulting from wave setup induces a barotropic pressure gradient, which partly drives a bed return flow or undertow (Garcez-Faria et al. 2000), which is one of the main processes responsible for coastal erosion.

The first theoretical explanation for the development of wave setup is due to Longuet-Higgins and Stewart (1964), who introduced the concept of radiation stresses, which correspond to the wind-generated wave momentum flux. In the near shore, the depth-limited dissipation of short waves causes a strong gradient of radiation stress, which acts as a horizontal pressure force toward the shore and tilts the water level until a balance is reached with the subsequent barotropic pressure gradient. As a result, the mean water level near the breaking point lowers (set-down) and the mean water level at the shoreline rises (setup). This wave-induced deformation of the water level was successfully reproduced in a wave channel by Bowen et al. (1968), as shown in Fig. 2.

2.2 Infragravity Waves

Infragravity (hereafter IG) waves are surface gravity waves with frequencies typically ranging from 0.004 to 0.04 Hz and related to the presence of groups in incident short waves (see Bertin et al. 2018 for a recent review). While IG waves are only a few millimeters to a few centimeters high in the deep ocean (e.g., Rawat et al. 2014; Crawford et al. 2015; Smit et al. 2018), they grow in the nearshore and their height can exceed 1 m at the shoreline (see Ruessink 2010; Sheremet et al. 2014; Fiedler et al. 2015; Inch et al. 2017). As a consequence, IG waves have a relevant contribution to the nearshore hydrodynamics, particularly under storm waves (e.g., Guza and Thornton 1982; Elgar et al. 1992; Ruessink et al. 1998).

Two main mechanisms typically explain the development of IG waves in the nearshore. First, the divergence of the momentum flux associated with the short waves at the scale of
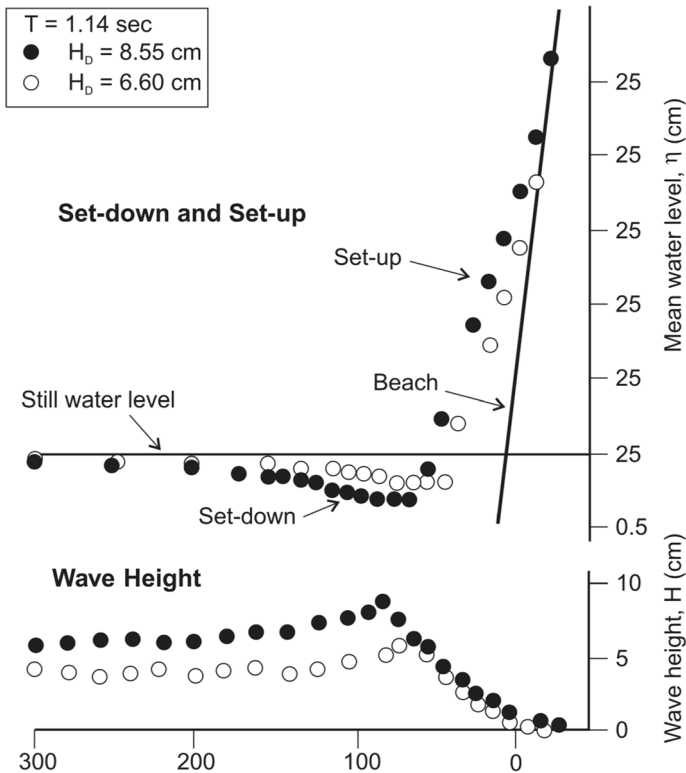
Fig. 2 Profile of the mean water level and the envelope of the wave height for two experiments of Bowen et al. (1968) with wave period = 1.14 s, H_s = 6.60 cm and H_s = 8.55 cm. Reprinted from Bowen (1969), as authorized by Wiley Online Library

wave groups drives the development of a long bound wave, out of phase with the energy envelope of the short waves (Biesel 1952; Longuet-Higgins and Stewart 1962). Has-selmann (1962) proposed an analytical solution to compute the bound wave for 2D random waves, which implies that the bound wave increases with the energy of the short wave, particularly when this energy is distributed over narrow-banded spectra. Second, due to the presence of wave groups, the cross-shore position of the breaking point varies in time and the equilibrium in the surf zone between the gradient of wave radiation stress and the sub-sequent barotropic pressure gradient becomes dynamic (see previous section and Fig. 1b). This process generates IG waves radiating from the breaking point seaward and shoreward (Symonds et al. 1982). Battjes et al. (2004) showed that the former mechanism is dominant at gently sloping beaches, while the latter is dominant in steep surf zones, such as in coral reefs (e.g., Pomeroy et al. 2012). However, a recent study of Moura and Baldock (2017) questioned these well-admitted findings and suggested that the breakpoint mechanism could also be dominant for wide surf zones under spilling breakers. Cheriton et al. (2016) and Gawehn et al. (2016) further showed that IG waves can trigger resonant processes in coral reefs, which result in the development of very-low-frequency motions.

In the surf zone, the dissipation of short waves through depth-limited breaking reduces their groupiness, so that IG waves are no longer bound and can propagate as free waves

(Battjes et al. 2004). In the inner surf zone, IG waves transfer the energy to higher frequencies, which results in their steepening and can lead to their dissipation by breaking, particularly at gently sloping beaches (Battjes et al. 2004; De Bakker et al. 2014). As beaches usually display a steeper profile in their upper part—called the berm—IG wave dissipation at high tide is reduced and IG waves can dominate the runup (Ruggiero et al. 2004; Fiedler et al. 2015). The IG wave energy that is not dissipated can be reflected offshore, where it can be trapped by refraction and promote the development of edge waves (Bowen and Guza 1978) or be leaked and propagate through the ocean with little dissipation (Rawat et al. 2014).

2.3 Wave Runup

When wind-generated waves reach the shores, they travel up (uprush) and down (backwash) the beach before being reflected seawards. This water displacement is called the swash, and the beach extent over which it occurs is the swash zone. The maximum vertical excursion of the waterline—called the wave runup—is usually measured with respect to the still water level, as for the wave setup. Therefore, the wave runup includes the contribution of both the swash and the wave setup. The swash energy is usually decomposed into a high-frequency band (incident band ~ 0.04 Hz–0.4 Hz) and a low-frequency band (infragravity band ~ 0.004 Hz–0.04 Hz). During extreme wave conditions, the wave runup can exceed 10 m (see Fig. 3; Poate et al. 2016). It is thus a key parameter for the design of coastal structures and the prediction of overtopping volumes

Fig. 3 Example of coastal defence overtopping at Chesil Beach, UK, caused by extreme swash events exceeding 10 m (see Poate et al. 2016) during Petra storm on February 5, 2014 (credits: Tim Poate)

during storm events. Given the strongly nonlinear nature of the wave-breaking process, the transition from undular bore to wave runup and the collision between uprush and backwash, analytical solutions have been derived for simplified cases only (e.g., Carrier and Greenspan 1958) and the cost of numerical simulations capable of representing such processes is often prohibitive for large-scale studies. Significant advances for the prediction of wave runup in natural environments stem from empirical approaches conducted either in the laboratory (Hunt 1959; Van der Meer and Stam 1992) or in the field (see Stockdon et al. 2006 for a description of major runup field experiments conducted between 1982 and 1997). These studies have shown that the wave runup mostly depends on the wave height (H), the wavelength (L) and the foreshore slope (β) (see Sect. 4.1.3 and Table 1 for a list of wave runup formulation). Since the wavelength scales with the square of the wave period in deep water, the wave period has actually a larger influence than the wave height on the runup. However, the range of wave period at a given site is usually lower than the range of wave heights, and this latter often display stronger correlations with the wave runup (Poate et al. 2016; Dodet et al. 2018). Several studies investigated more closely the spectral distribution of the wave energy in the swash zone and revealed that the energy in the incident band could be saturated in dissipative environments, such as high-energy low-sloping beaches, so that infragravity wave energy was dominant (Ruessink et al. 1998). In order to investigate the impact of the foreshore slope on the wave runup, some authors took advantage of the strong alongshore variability of sandy beaches (Ruggiero et al. 2004) or the large tidal range that modifies the foreshore morphology felt by the waves (Suanez et al. 2015), or carried out interfield comparisons (Stockdon et al. 2006). These studies show a significant impact of the foreshore slope on the runup for reflective conditions and a lesser or nonexistent impact for high-energy dissipative environments.

In this section, we have seen that wave-induced coastal processes have a significant impact on coastal sea level. All these processes are largely controlled by offshore wave conditions. Therefore, given the strong variability of the offshore wave climate at various timescales (seasonal, interannual, decadal) and its potential long-term evolution

Table 1 Wave setup (η) empirical formulations (non-exhaustive list)

References	Empirical equation	Applicability range
Guza and Thornton (1981)	$\eta = 0.17 H_s$	
Holman and Sallenger (1985)	$\eta = 0.46 \tan \beta \sqrt{H_s L_0}$	$0.026 < \beta < 0.14$
Holman (1986)	$\eta = 0.2 H_s$	$0.07 < \beta < 0.2$
Hanslow and Nielsen (1992)	$\eta = 0.048 \sqrt{\dfrac{H_s}{\sqrt{2}} L_{0,s}}$	$0.03 < \beta < 0.16$
Komar (1998)	$\eta = 0.45 \tan \beta \sqrt{H_0 L_0}$	$0.026 < \beta < 0.14$
Hedges and Mase (2004)	$\eta = 0.34 H_s$	$\xi_s < 3$
Stockdon et al. (2006)	$\eta = 0.35 \beta \sqrt{H_0 L_0}$	$\xi_0 > 0.3$
Stockdon et al. (2006)	$\eta = 0.016 \sqrt{H_0 L_0}$	$\xi_0 < 0.3$
Atkinson et al. (2017)	$\eta = 0.16 H_s$	Model of models
Ji et al. (2018)	$\eta = 0.220 H_s^{0.629} L_0^{0.371} (\tan \beta)^{0.538}$	$0.005 < \beta < 0.10$

β is the foreshore beach slope, H_s is the deep-water significant wave height, H_0 is the deep-water wave height, L_0 is the deep-water wavelength $L_{0,s}$ the deep-water wavelength computed using the significant period

in the context of climate change, it is particularly important to better understand past and future changes in wave conditions and how these changes will translate in terms of coastal sea level.

3 Characterization and Variability of Offshore Wave Conditions

Since the first evidence of long-term changes in significant wave height measured by the Sevenstones Lightship wave recorder 25 km off Cornwall Land's End (UK) (Carter and Draper 1988), significant progress has been achieved on our comprehension of past and future evolution of the wave climate. Part of this progress can be attributed to the deployment and maintenance of large-scale buoy networks, the development of numerical models and the advent of satellite Earth Observation programs. In this section, we first describe the different methods that are used to characterize offshore wave conditions. Then, we present the current state of the art regarding past and future evolution of the wave climate at global scale, based on the IPCC 5th Assessment Report (AR5; chapter 3, Rhein et al. 2013 and chapter 13, Church et al. 2013) and the Special Report on Managing the Risks of Extreme Events and Disasters to Advance Climate Change Adaptation (SREX; chapter 3, Seneviratne et al. 2012) as well as more recent findings published since AR5.

3.1 In situ and Remote Sensing Observations of Offshore Wave Conditions

Wave measurements started with visual observations from the coast using a wind sea and swell separation method and estimations of wave heights and periods (Gain 1923; Munk and Traylor 1947). Such visual observation programs continue for offshore ship-based observations (e.g., Gulev et al. 2003), providing the longer time series of wave measurements (Gulev and Grigorieva 2004). Offshore of the surf zone and in regions where currents are under 1 m/s, the most common source of wave measurements is moored surface following buoys based on accelerometers (Longuet-Higgins et al. 1963; Allender et al. 1989) or GPS velocity measurements (Herbers et al. 2012). Although not coordinated under a single international program, the collection of wave buoy data has been facilitated by the Oceansites program (Send et al. 2010), as well as various efforts associated with the Global Ocean Observing System (GOOS) and the Copernicus Marine Environment Monitoring System (CMEMS). The actual response of the buoy to the water motion depends on the hull shape and sensor mounting (Jensen et al. 2015; Guimaraes et al. 2018). Where currents are strong. Acoustic Doppler current profilers (ADCPs) are interesting alternatives to measure both currents and waves (Herbers and Lentz 2010), and drifting surface buoys can also provide interesting information either with dedicated buoys (Thomson et al. 2012), or with motion packages added on drifters from the Global Surface Velocity Program (Lumpkin et al. 2016). In that context, in situ wave measurements are today provided by hundreds of wave buoy moored in both deep or coastal waters (typically in 15–100 m depth), with most time series extending over 20 to 40 years (e.g., US National Data Buoy Center, https://www.ndbc.noaa.gov/). These measurements cannot give the detailed wave information needed to estimate coastal sea levels, in particular over complex shorelines due to wave evolution outside of the surf zone, mostly due to refraction (Munk and Traylor 1947; Magne et al. 2007) and bottom friction (e.g., Ardhuin et al. 2003; Roland and Ardhuin 2014). Also, buoys do not measure the full directional spectrum, but moments of its
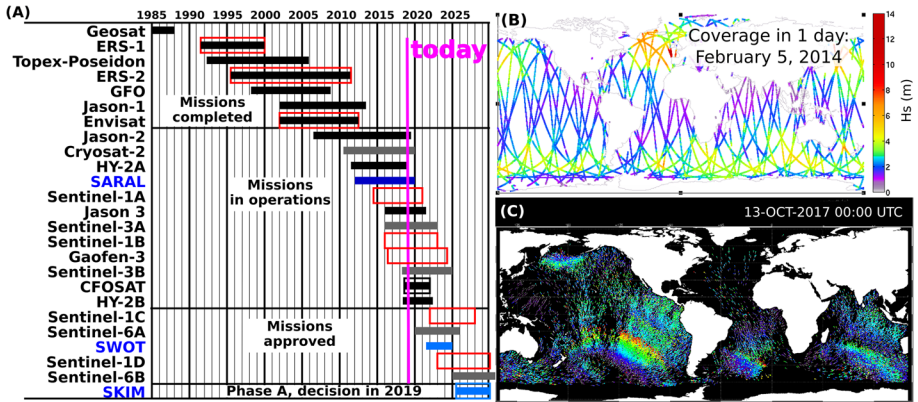
Fig. 4 a Time coverage of satellite missions from 1985 to 2030, including nadir and near-nadir altimeters (solid bars) missions monitoring ocean wave spectra (open box) using C-band Synthetic Aperture Radars (red), and real aperture radars in Ku-band (black) or Ka-band (blue). The light gray bars correspond to altimeters using delay Doppler processing. **b** Example of 1-day coverage for H_s measurements with four satellite altimeters, **c** snapshot of "fireworks," showing peak periods, and heights of swell partitions derived from Sentinel-1A and Sentinel-1B wave mode data. Reprinted from Ardhuin et al. (2019), as authorized by Frontiers copiright statements

distribution, that lead to important uncertainties when waves are propagated to the coast (e.g., Crosby et al. 2017).

A more complete spatial coverage of ocean waves is provided by satellite remote sensing, as illustrated in Fig. 4. Nowadays, satellites provide most of the background data for wave climatologies and detection of trends. Satellite altimeters, particularly, give an uninterrupted record of significant wave height since the launch of ERS-1 in 1991. Additional information on the sea state, in particular wave periods that are critical for estimating wave-induced water levels at the coast, can be obtained with other satellite remote sensing techniques. In particular, ERS-1, ERS-2, Envisat and the Sentinel 1 constellation carry synthetic aperture radars (SARs) that are operated in "wave mode" over most of the oceans (Hasselmann et al. 2012). SAR provides radar images from which the height, period and direction of swells can be estimated, provided that their wavelength is long enough, typically more than 200 m depending on their direction and on the wind speed (Kerbaol et al. 1998). Both altimeter H_s and SAR-derived swell partitions are assimilated into the CMEMS/Meteo-France operational global model (Aouf et al. 2006), which today provides the most accurate forecasts of wave heights (Bidlot 2017), with the swell assimilation impact strongest in the Pacific ocean.

3.2 Regional Modeling of Offshore Wave Conditions

Given the difficulty of monitoring waves over large spatial and temporal scales, numerical models are important tools, often combined with in situ measurements and remote sensing. A wide range of numerical techniques exist, each adapted to particular scales and physical processes to be accounted for (see Ardhuin and Orfila 2018 for a recent review). As long as time resolution shorter than the wave group scale (a few minutes) is not needed, the flow, water level and wave motion can be separated, and the waves are efficiently solved
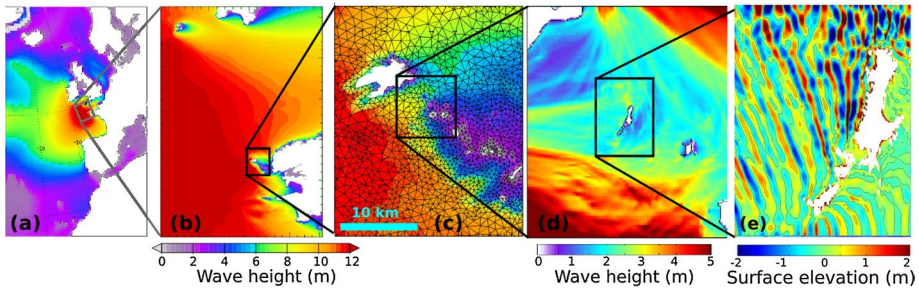
Fig. 5 Example of multiple scales wave modelling. **a–c** Phase-averaged wave model (WAVEWATCH III, the WAVEWATCH III Development Group 2016), **d** wave-group-resolving model (XBeach, Roelvink et al. 2018), and **e** phase-resolving wave model (SWASH, Zijlema et al. 2011), here applied at Banneg Island, France

with spectral wave models that are generally phase-averaged (e.g., the WAVEWATCH III Development Group 2016) and that may also include a bispectrum evolution for taking into account non-local nonlinear effects (Herbers and Burton 1997; Janssen et al. 2006). Spectral phase-averaged models can be applied at all spatial scales (Fig. 5).

Numerical models can provide good wave prediction, but are computationally time-consuming. Meta-models (also called "response surface", "surrogate model", "model emulators", "proxy models") provide an alternative approach to tackle the computation time issue. They are based on the definition of a statistical relationship between the inputs (X, called the "predictor") and the output (Y, called the "predictand"). Such fast-running model allows, for instance, performing sensitivity analysis, exploring the effect of uncertainties in X on the Y results, or performing ensemble simulations. From the literature review, wave meta-models can be divided into two categories (statistical downscaling (SD) and hybrid (H) models), the first one being the one used when investigating waves at a regional scale. Local waves resulting from the regional meteorology over a few days scale (Camus et al. 2014a), the SD models relate a large-scale predictor (most of the time the sea-level pressure fields or its squared gradient) with a local predictand (multivariate wave conditions, e.g., wave height, period and direction). They require atmospheric and sea-state databases. One of the key points in statistical downscaling is to reduce the dimension of the inputs, i.e. here the mean sea-level pressure (or its gradient), which has very high dimension (number of grid points times the number of time steps). This reduction is often based on principal component (PC) analysis. Then, two types of approaches have been pursued. In the first one, the SD model is defined as a linear combination of the most important PCs of the predictor defined specifically for the analyzed target location (see e.g., Camus et al. 2014a). In the second one, the SD model estimates the predictand based on the occurrence of weather types (see, e.g., Camus et al. 2014b, Laugel et al. 2014; Perez et al. 2015; Rueda et al. 2016). These weather types are obtained by clustering methods (e.g., K-means), initialized by a maximum dissimilarity algorithm. In many studies, a typical number of 100 weather types are used. Then, a regression model is built between these weather types and the wave conditions. At the end, a statistical model is built allowing emulation of the wave conditions with a negligible computation time. However, although revealing the dominant modes of wave climate variability and trends, the statistical downscaling methods still faces issues to predict extremes at high frequency (e.g., hour scale). It should be noted that statistical downscaling models aiming at predicting cyclone-induced wave conditions rely

on the cyclone characteristics rather than on spatiotemporal meteorological fields (see, e.g., Jia and Taflanidis 2013; Rohmer et al. 2016).

3.3 Past Changes in Wave Conditions During the Twentieth Century

Buoy data and Voluntary Observing Ship (VOS) reports indicate statistically significant positive H_s trends during the second half of the twentieth century over the North Atlantic, north of 45°N, and over the central to eastern mid-latitude North Pacific with typical trends of up to 2 cm per year, as shown in Fig. 6a (Gulev and Grigorieva 2006; Ruggiero et al. 2010). However, these measurements suffer from limited spatial coverage, particularly in the Southern Ocean. In addition, some of the trends computed from the North Pacific buoy data were introduced by modifications of the measurement techniques (Gemmrich et al.
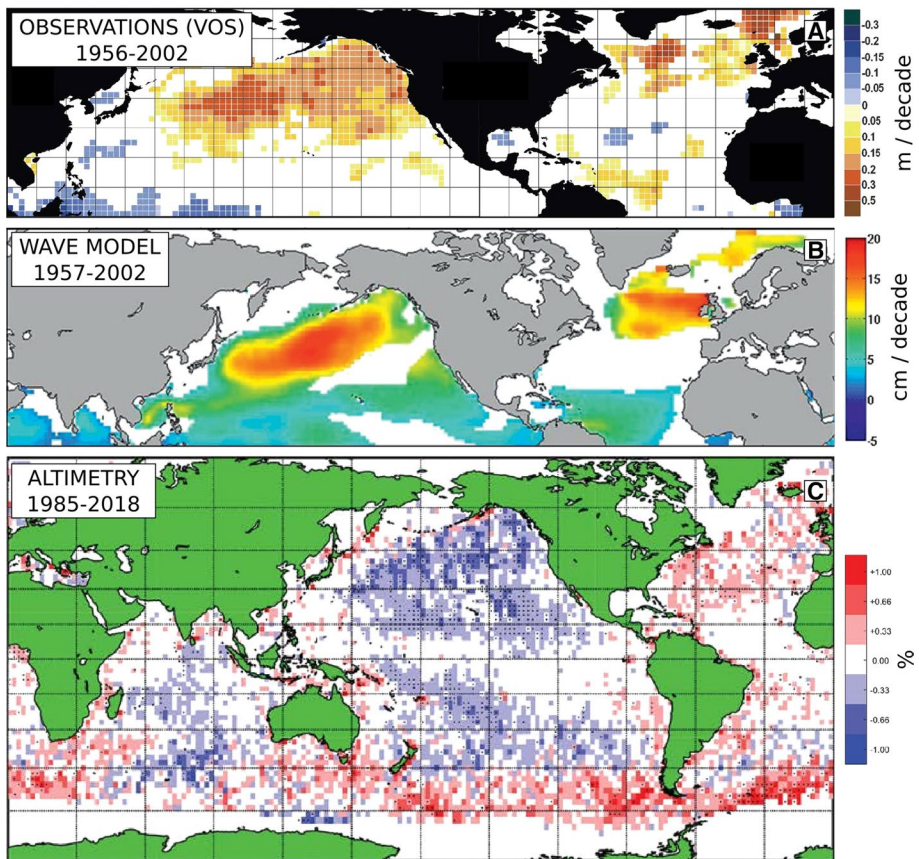
Fig. 6 Trends in significant wave height estimated from **a** visual observing ship observations over the period 1956–2002. Reprinted from Gulev and Grigorieva (2006), © American Meteorological Society. Used with permission; **b** numerical wave model hindcast over the period 1957–2002. Reprinted from Semedo et al. (2010), © American Meteorological Society. Used with permission; **c** satellite altimetry over the period 1985–2018. Reprinted from Young and Ribal (2019), with permission of AAAS. In each of these studies, values which are not statistically significant are either not shown (**a** and **b**) or not marked with black dots (**c**). Adapted from Gulev and Grigorieva (2004), Semedo et al. (2010) and Young and Ribal (2019)

2011). For these reasons, satellite altimeter observations available since the mid-1980s provide extremely valuable data source for investigating wave height variability at global scale. Using an extensive altimetry database, Young and Ribal (2019) found positive trends (up to 0.5 cm per year) for the mean annual H_s in some part of the Southern Ocean and negative trends in the central part of the North Pacific, with a global low level of statistical significance (Fig. 6c). They also obtained stronger positive trends (up to 1 cm per year) for the 99th H_s percentile in the Southern Ocean, North Atlantic and North West Pacific. Given the short time period covered by the data (1985–2018) and the strong link between variations in waves and internal climate variability, it is yet difficult to determine whether these results reflect long-term H_s trends or are a part of the decadal oscillation. The differences observed between the trends computed over the period 1985–2018 from satellite altimetry and the ones computed over the period 1957–2002 from observations and model results (compare Fig. 6a–c) also illustrate how the internal atmospheric variability may impact the H_s trends computed over a few decades.

Numerical wave hindcasts forced by general circulation models (GCMs) or regional climate model (RCM) reanalysis offer an additional alternative to study wave climate variability over a longer time period with a high resolution and global coverage, even though temporal inhomogeneity in the reanalysis data limits the confidence in the model results for long-term trend analysis (e.g., Stopa et al. 2019). A 45-year (1957–2002) hindcast forced by the ERA-40 reanalysis from the European Centre for Medium-Range Weather Forecasts (ECMWF) revealed positive H_s trends in the North Atlantic and North Pacific similar to the one obtained from in situ measurements (Semedo et al. 2010, Fig. 6b). Hemer et al. (2010) obtained positive trends across most of the Southern Hemisphere using a corrected ERA-40 reanalysis and showed that winter H_s was strongly correlated with the SAM. They also found an anticlockwise rotation of wave direction with the southward intensification of the Southern Ocean storm belt associated with the southern annular mode (SAM). In the North Atlantic, Dodet et al. (2010) found positive H_s trends (up to 15 cm/decade) north of 40°N and clockwise trends (up to 1°/decade) in mean wave direction south of 45°N during the period 1953–2009. They related these changes to a strengthening and northward shift of mid-latitude storms associated with changes in the North Atlantic Oscillation (NAO) that shifted from a negative phase in the 1960s to a positive phase in the 1990s. These results are consistent with the 1958–2002 wave hindcast of Charles et al. (2012). Bertin et al. (2013) performed a 109-year numerical wave hindcasts for the North Atlantic and found significant upward trends in yearly-mean H_s in the North-East Atlantic, reaching 10 cm/decade around 60°N, despite any trends in NAO over the same period. This upward trend was explained by an upward trend in 10-m winds, observed both in atmospheric hindcast and in observations from VOS (Gulev et al. 2003). More recently, Castelle et al. (2018) performed a wavelet analysis in a 69-year (1949–2017) wave hindcast in the North-East Atlantic and found an increase in H_s variability starting in the 1990s, that is also observed in the pressure-based index. In the Arctic Ocean, reduction in summer sea ice extent resulted in enhanced wave activity due to increased fetch area and longer duration of the open water season (Overeem et al. 2011; Stopa et al. 2016).

3.4 Projected Changes for the End of the Twenty-First Century

Given the usually coarse resolution (typically 250 km) of the atmospheric component of global coupled atmosphere–ocean general circulation model (GCM), global wave climate projections usually require dynamical (Wang and Swail 2006) or statistical (Camus
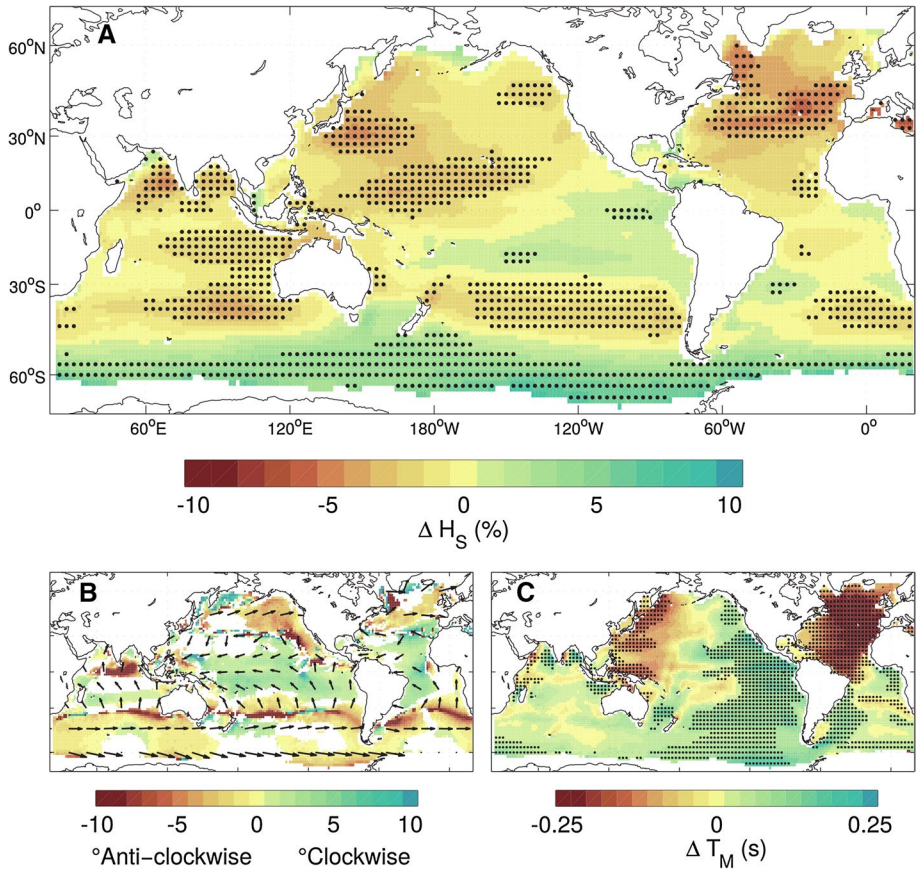
Fig. 7 Projected changes in wind-wave conditions (~ 2075–2100 compared with ~ 1980–2009) derived from the Coordinated Ocean Wave Climate Projection (COWCLIP) Project (Hemer et al. 2013a). **a** Percentage difference in annual mean H_s. **b** As for **a**, but displaying absolute changes in mean wave direction, with positive values representing projected clockwise rotation relative to displayed vectors, and colours shown only where ensemble members agree on the sign of change. **c** As for **a**, but displaying absolute changes in mean wave period. The symbol ~ is used to indicate that the reference periods differ slightly for the various model studies considered. Adapted from Church et al. (2013)

et al. 2017) downscaling approaches to increase the resolution of the forcing wind fields. Hemer et al. (2013a) analyzed the results of an ensemble of four dynamical and one statistical wave models developed as part of the Coordinated Ocean Wave Climate Project (COWCLIP) and compared the averaged multimodel wave parameters for the time-slice 2070–2100 with the ones for the time-slice 1979–2009 (Fig. 7). They found a statistically significant decrease in the annual H_s for 25.8% of the global ocean area and a statistically significant increase for 7.1% of the global ocean, predominantly in the Southern Ocean. These trends were more pronounced when focusing on the winter mean. The increase in wave activity in the Southern Ocean was shown to affect the wave period and wave direction in the other ocean basins, with a clockwise rotation of the wave direction in the tropics and larger wave periods in the eastern Pacific, as a result of enhanced wave generation in the Southern Ocean and northward swell propagation. In the North

Atlantic and North Pacific, a significant decrease in H_s and wave period is associated with weaker wind forcing projected in these regions. Wang et al. (2014) used a statistical model to derive project changes in H_s from changes in the sea-level pressure fields of 20 CMIP5 simulations. They obtained trend patterns similar to previous analysis, but also noted some differences with the results of studies based on CMIP3 GCM (Hemer et al. 2013a). For instance, they found a much more extensive H_s increase in the tropical South Pacific and an opposite H_s trend (increasing instead of decreasing) in the tropical South Atlantic, compared to Hemer et al. (2013a). Mentaschi et al. (2017) computed the projected changes in wave energy fluxes (integrating both H_s and the wave period) from the results of a wave model forced by an ensemble of five CMIP5 GCM models. They found a significant increase up to 30% in the 100-year return level for the majority of the coastal areas of the southern temperate zone and significant negative trend in large areas of the northern hemisphere. They explained these trends in extreme wave energy fluxes (WEFs) by the intensification of teleconnection patterns such as the Arctic Oscillation (AO), the El-Nino Southern Oscillation (ENSO) and the NAO. Casas-Prat et al. (2018) investigated the future wave projections in the Arctic using an unstructured spherical grid wave model forced with the wind fields and ice concentration of five CMIP5 GCM models. They found that by the end of the twenty-first century the wave climate in the Arctic region will be significantly different compared to the current climate due to ice retreat yielding new open water areas for wave generation. In particular, their ensemble projected mean H_s changes to reach 1.75 m by the end of the twenty-first century in newly open water. In the historical open water areas, the ensemble average projected some significant increases (up to 15%) in the Barents Sea, which can be related to the local increase in surface wind.

In summary, offshore wave conditions show strong spatial and temporal variability, which can be related to large-scale patterns in the atmospheric circulation. Although most available wave data are too short or overly inhomogeneous to clearly depict past long-term trends, most studies agree on significant positive H_s trends of the order of ~ 1 cm/year in the North Atlantic and Southern Ocean. In contrast, model projections for the end of the century tend to agree on a significant decrease in H_s in the North Atlantic and a significant increase in the Southern Hemisphere, but show contrasting results in other ocean basins such as the South Atlantic, the Indian Ocean or the North Pacific (Morim et al. 2018). In the following section, we will see how such changes may impact coastal sea level and add to ocean dynamic sea-level rise.

4 Wave Impacts on Coastal Sea Level

Measuring ocean properties in the nearshore environment is a challenging task. Contrary to deep-water environments, the nearshore bottom topography plays a fundamental role in the ocean dynamics, through refraction, diffraction, frictional, shoaling, breaking and resonant processes. Hence, the observed variability of most physical ocean parameters (wave height, sea level, currents) cannot be investigated without knowledge on the bottom topography, which is hardly available and may evolve rapidly. Also, the strong gradients in the bottom topography, currents and wave properties, which characterize the nearshore zone, often preclude the application of large-scale remote sensing techniques and coarse-resolution modelling strategy. Finally, the strong wave energy

dissipation that occurs when wave break in the nearshore (see Sect. 2) makes the surf zone a very dynamic area with strong currents and rapid topographic changes, where long-term deployment of in situ measurements is very complicated. For these reasons, our knowledge on coastal sea level mostly relies on a few tide gauge time-series partly sheltered from the effect of wave and is therefore very limited compared to our knowledge on offshore sea-level changes. In this section, we present the current techniques used to measure and model nearshore topography, wave and sea level. Then, we discuss the impact of waves on coastal sea level based on recently published studies.

4.1 Topography, Waves and Sea Level in the Nearshore

#### 4.1.1 Observation Techniques

Important nearshore observation programs have been developed in Australia, Europe or in the USA, with long-term monitoring of beach topography, nearshore wave conditions and water level that now extend over 30 years, but only at a few dedicated locations. The US Army Corps of Engineers Field Research Facility, located in Duck, North Carolina, is one of these sites with a continuous detailed monitoring of offshore and nearshore directional wave spectra, beach profiles and daytime video monitoring of the nearshore and intensive process studies (Birkemeier 1997; Holman and Stanley 2007). The Petten dike in the Netherlands (Wenneker et al. 2016), Narrabeen beach in Australia (Turner et al. 2016) or Truc Vert beach in France (Castelle et al. 2014) are other examples of coastal locations dedicated to long-term monitoring survey. At these sites, observations of sea level right at the shoreline have been combined with measurements of waves and nearshore topography to produce empirical parameterizations (see Sect. 4.1.3), suggesting that observing surf zone topography and waves outside of the surf zone could be a first step to extrapolate regional-scale storm surge levels all the way to sea levels right at the coast.

Close to the shoreline and across the surf zone, pressure-based systems have been developed (Barber et al. 1946; Munk et al. 1963) and are still widely used to measure the wave spectrum, giving the distribution of the surface elevation variance as a function of frequency, with recent improvements to correct for nonlinearities in the transformation from bottom pressure to surface elevation (Bonneton et al. 2017). Pressure is often combined with velocity measurements to provide a measurement of wave propagation direction as well as currents (e.g., Thornton and Guza 1983). Other instruments used routinely from structures include runup gauges (Wenneker et al. 2016) and shore-based video systems (Holman and Haller 2013). With the progress made on estimating variables from video imagery, such as wave height, sea level and runup, and morphology, this technique offers now access to an unequaled high frequency (hourly) and long-term description of the nearshore dynamics (Pianca et al. 2015; Almar et al. 2017; Brodie et al. 2018) including bathymetry (Holman et al. 2013; Bergsma and Almar 2018) and sea level (Abessolo Ondoa et al. 2019). The installation of shore-based video stations to monitor the nearshore is increasingly used due to their possibilities and low cost. Combining these video techniques with the use of unmanned aerial vehicle (UAV) has also greatly enlarged the scope of application of these methods (e.g., Turner et al. 2016; Matsuba and Sato 2018). Although video is limited to daytime monitoring, the development of LIDAR technology is expanding the possibilities of shore-based remote sensing (Blenkinsopp et al. 2010; Almeida et al. 2015; Brodie et al. 2015) and now offers an
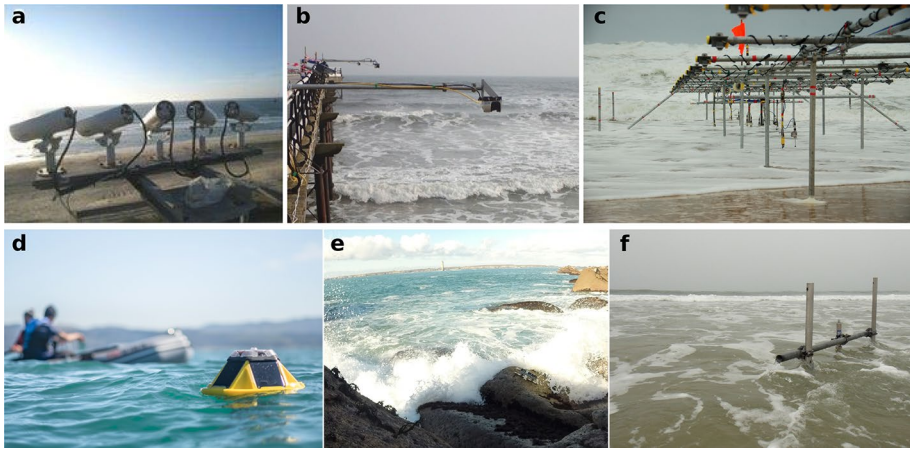
Fig. 8 **a** Video camera system overlooking Biscarrosse beach, France (Marchesiello et al. 2015); **b** LIDAR scanner array fixed along a pier at Saltburn beach, UK (Martins et al. 2017); **c** array of ultrasonic sensors measuring swash and bed elevations at Truc Vert beach, France (Masselink et al. 2009, credits: Tim Scott); **d** wave buoy spotter; **e** pressure sensors installed on the rocky cliffs of Banneg Island, France (Dodet et al. 2018); **f** PUV system (pressure and current meter) partially immersed on the ebb shoal of the Obidos lagoon, Portugal (Bruneau et al. 2011)

attractive alternative to monitor high-frequency topography and runup or more recently, the detailed geometric properties of waves in the surf zone (Martins et al. 2018). First long-term deployments are being conducted (e.g., at Narrabeen, Australia) and should provide soon new insights in the quantification of multiscale runup dynamics and flooding events (Almeida et al. 2018). Combining measurements from shore-based lidars and
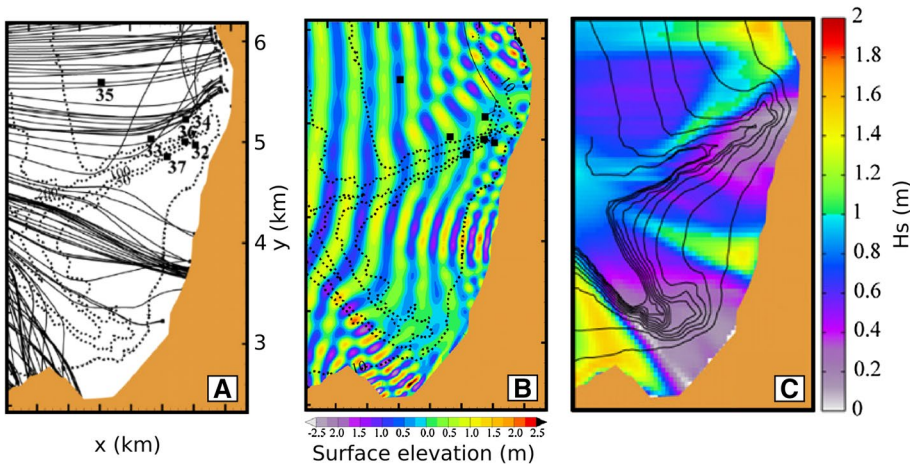
Fig. 9 Different representations of wave propagation over the Scripps-La Jolla submarine canyons. **a** Wave rays for 15 s with a constant offshore direction from the West and an offshore spacing of 20 m. **b** Solution of the mild slope equation for 1 m amplitude 15 s monochromatic swells, with a phase-resolving model. **c** Significant wave height computed for 15 s swells from the West with a phase-average spectral model. Reprinted from WISE Group (2007), as authorized by Elsevier

from tide gauges might allow to separate observed wave setup and runup from offshore sea-level variability. However, all these measurements are very localized and give a very partial view of the complex spatial patterns in waves and associated water levels. Figure 8 shows several instruments used to measure nearshore parameters.

4.1.2 Numerical Models

Spectral phase-averaged models are typically only limited by their poor representation of diffraction effects (e.g., Holthuijsen et al. 2003), which are typically negligible on natural topographies (e.g., Fig. 9 and Magne et al. 2007). In small areas, the effect of local winds may be neglected and backward ray tracing can be a very efficient linear model (O'Reilly and Guza 1993; Crosby et al. 2017). Phase-resolving models can also be used to better represent steep topographies and associated diffraction, as well as nonlinear shoaling effects; however, in their time-stepping version they can be prohibitively expensive in computation time for regions larger than about 10 km and timescales beyond a few hours. However, a great advantage of such models is that they solve the full flow, including water-level variations and currents, allowing the representation of rapid couplings, for example, in the swash zone, including inundation (e.g., Chen et al. 2002; Zijlema et al. 2011; Torres-Freyermuth et al. 2013).

Ocean circulation models (either based on the shallow water or the primitive equations) can be forced by phase-averaged forces to represent the wave effect on the mean sea level and the setup. This approach is generally successful except in very shallow water (Apotsos et al. 2007). Numerous coupled wave-current models have been developed in the last decade with some applications to coastal water levels (e.g., Walstra et al. 2000; Ozer et al. 2000; Kumar et al. 2012; Bennis et al. 2014; Stockdon et al. 2014; Cohn and Ruggiero 2016; Guérin et al. 2018). For depth-integrated motions, waves contribute to a horizontal force, that is usually represented by the divergence of a horizontal radiation stress tensor (Longuet-Higgins and Stewart 1964; Smith 2006). When vertical profiles of the current are considered, it is most convenient to write the equations for the flow momentum only (McWilliams et al. 2004; Ardhuin et al. 2008a, b, c; Suzuki and Fox-Kemper 2016).

The effect of infragravity waves has for long remained unaccounted for in wave-current models. However, the devastating impact of several hurricanes on the sandy coasts of Florida in 2004 has triggered the development of a new modeling approach to simulate water-level changes during storms including the effect of IG waves. The XBeach modelling system (Roelvink et al. 2009) uses this so-called surfbeat approach and couples a depth-integrated flow model with a spectral wave model, which represents the short-wave groups. IG waves can also be represented using phase-resolving models (e.g., Zijlema et al. 2011; Bonneton et al. 2011), although the large associated computational time limits such approach to domains a few km-large at maximum.

4.1.3 Empirical Models

Wave setup and runup cannot yet be modelled at large spatial scales (regional to global) with numerical hydrodynamic models or over the long periods needed to study, for instance, their contribution to water-level extremes (statistically) and their evolution under climate change, as they would need high-resolution mesh, knowledge of the full incident wave spectra and of nearshore morphology. To overcome these difficulties, empirical

Table 2 Wave runup empirical formulations (non-exhaustive list)

References	Empirical equation	Applicability range
Wassing (1957)	$R_{2\%} = 8\tan\beta H_{st}$	$0.05 < H/L < 0.07$
Hunt (1959)	$R_{2\%} = \tan\beta\sqrt{H_0 L_0}$	
Holman and Sallenger (1985)	$R_{2\%} = 0.92\tan\beta\sqrt{H_s L_0}$	$0.026 < \beta < 0.14$
Holman (1986)	$R_{2\%} = 0.2H_s + 0.83\tan\beta\sqrt{H_s L_p}$	$0.07 < \beta < 0.2$
Mase (1989)	$R_{2\%} = 1.86 H_0 \xi_s^{0.71}$	$0.03 < \beta < 0.2\ 0.007 L_0 < H_0$
Powell (1990)	$R_{2\%} = H_s\left[2.86 - 62.69\left(\frac{H_s}{L_0}\right) + 443.29\left(\frac{H_s}{L_0}\right)^2\right]\left(\frac{-\ln 0.02}{4.2}\right)^{0.455}$	Gravel beaches, $H_s < 5$ m
Nielsen and Hanslow (1991)	$R_{2\%} = SWL + 1.98*0.042\sqrt{H_s L_{0,s}}$	$\beta < 0.10$
	$R_{2\%} = SWL + 1.85*0.052\tan\beta\sqrt{H_s L_{0,s}}$	$\beta < 0.10$
Van der Meer and Stam (1992)	$R_{2\%} = 1.5\tan\beta\sqrt{H_{st}L_p}$	$0.5 < \xi_p < 2$
Ruggiero et al. (2001)	$R_{2\%} = 0.27\sqrt{\beta H_s L_p}$	$0.005 < \beta < 0.025$
Hedges and Mase (2004)	$R_{2\%} = 0.34H_s + 1.49\tan\beta H_s L_0$	$\xi_s < 3$
Stockdon et al. (2006)	$R_{2\%} = 1.1\left[0.35\beta\sqrt{H_s L_p} + 0.5\left(H_s L_p\sqrt{0.563\beta^2 + 0.004}\right)\right]$	$\xi_0 > 0.3$
Stockdon et al. (2006)	$R_{2\%} = 0.043\sqrt{H_s L_p}$	$\xi_0 < 0.3$
Pullen et al. (2007)	$R_{2\%} = 1.65\tan\beta\sqrt{H_{m0}L_0}$	Dikes (of outer slope α)
Roberts et al. (2010)	$R_{2\%} = 1.00 H_b$	$\xi_0 > 0.3$
Vousdoukas et al. (2012)	$R_{2\%} = 0.53\beta\sqrt{H_s L_p} + 0.58\tan\beta H_s + 0.45$	Reflective beaches
Poate et al. (2016)	$R_{2\%} = 0.21 D_{50}^{-0.15}\sqrt{\tan\beta H_s T_{m-1m0}}H_s$ simplified to: $R_{2\%} = 0.49\sqrt{\tan\beta T_0 H_s}$	Gravel beaches $0.05 < \tan\beta < 0.20$
Atkinson et al. (2017)	$R_{2\%} = 0.92\tan\beta\sqrt{H_s L_p} + 0.16 H_s$	Model of models

β is the foreshore beach slope. Ω is the Dean parameter (Dean 1977), SWL is the still water level (see Nielsen and Hanslow 1991). ξ_s is calculated with respect to the deep-water significant wave height (H_s) and significant period (T_s). ξ_p corresponds to the Iribarren number calculated using the peak period and significant wave height. H_{st} is the significant wave height and H_{m0} is the wave height at the toe of the slope (for structures such as dikes), L_p is the peak period deep-water wavelength, L_0 the deep-water wavelength $L_{0,s}$ the deep-water wavelength computed using the significant period. H_0 is the deep-water wave height. D_{50} is the median sediment size

parameterizations have been developed based on observations collected during field or laboratory experiments to estimate wave setup and runup for natural beaches and artificial structures.

Most studies have shown that the wave setup and the wave runup mostly depend on the offshore wave height (H_0), the offshore wavelength (L_0) and the foreshore slope ($\tan\beta \sim \beta$), and can be expressed as a function of the Iribarren number $= \tan(H_0/L_0)^{-0.5}$ (Iribarren and Nogales 1949), also known as the surf-similarity parameter (Battjes 1974). The most common scaling for runup is that of Hunt (1959), where runup is proportional to $\xi_0 H_0$, which is equal to $\tan\beta(H_0L_0)^{0.5}$. A non-exhaustive list of the most commonly used empirical formulations of setup and runup can be found in Tables 1 and 2, respectively, and in the references therein. A list of empirical swash formulations can be found in Passarella et al. 2018. Note that the definition of the beach slope is not straightforward for complex profiles (e.g., concave profiles, presence of sandbars, rocky cliffs time-evolving bathymetry), but on natural beaches, the value of β is often taken as the foreshore slope, in the region covered by the swash (Stockdon et al. 2006). The foreshore beach slope can substantially vary in time and alongshore and has been poorly measured so far. As the dependence of runup to the coastal morphology is stronger for non-dissipative beaches, several empirical formulations for runup were also derived without a dependence to the beach slope, to be applicable to dissipative beaches only (e.g., Mase 1989; Holman and Sallenger 1985; Powell 1990; Nielsen and Hanslow 1991; Stockdon et al. 2006; Roberts et al. 2010; Table 2).

Existing wave setup, swash or runup formulations were extensively tested (e.g., Atkinson et al. 2017; Di Luccio et al. 2018; Senechal et al. 2011; Vousdoukas et al. 2012; Cohn and Ruggiero 2016; Díaz-Sánchez et al. 2014; Stockdon et al. 2014; Passarella et al. 2018; Ji et al. 2018; Pullen et al. 2007; Power et al. 2019). Although most of these formulae have significant skills, the scatter between predicted and observed setup or runup can be substantial. This could be due to second-order processes (e.g., edge waves, variability of the beach slope, nearshore morphological control on runup that is not captured when only accounting for the beach slope) that are not represented by the formulations' predictors (e.g., Díaz-Sánchez et al. 2014). In addition, empirical setup and runup formulations have been calibrated and/or validated with short observational time series, and Power et al. 2019 showed that they are prone to significant errors when applied outside the range of conditions over which they have been calibrated. Finally, empirical setup and runup formulations have mostly been developed for natural sandy beaches, which are among the most vulnerable environments to sea-level changes (Wong et al. 2014) and cover a large fraction of the world's coast (Luijendijk et al. 2018). However, wave setup can exist in other coastal environments such as semi-enclosed bays, harbors (Thompson and Hamon 1980), rocky cliffs (Dodet et al. 2018) or steep-shelf small islands with fringing reefs (see, e.g., Merrifield et al. 2014). Some processes that may be negligible for sandy beaches may dominate in such environments. Recent experiments conducted on gravel beaches (Poate et al. 2016) and rocky cliffs (Dodet et al. 2018) have revealed the significant role of beach grain size, bottom roughness and water infiltration within fractured bedrock on the wave runup propagation. Therefore, research efforts are still actively ongoing to improve existing formulations for setup, swash and runup (e.g., Atkinson et al. 2017; Power et al. 2019; Ji et al. 2018; Passarella et al. 2018) and to cover other coastal environments including structures (e.g., van der Meer 1992; Pullen et al. 2007) and gravel beaches (e.g., Poate et al. 2016).

4.1.4 Hybrid Models

In comparison with the statistical downscaling models presented in Sect. 3.2, the hybrid models are more focused on a local scale as they propagate hydrodynamic conditions. They combine statistical techniques and numerical models. They have been used to predict nearshore wave conditions, wave runup or water level at the coast, based on offshore hydrodynamic conditions (see, e.g., Camus et al. 2011; Gouldby et al. 2014; Rohmer and Idier 2012; Gainza et al. 2018; Passarella et al. 2018). These hybrid models rely on the interpolation of process-based simulations or observations. In the former case, the first step is to define the process-based simulations to run (using, for instance, maximum dissimilarity algorithm as in Gainza et al. (2018); or adaptive sampling as in Rohmer and Idier (2012). For the interpolation, it can be done, for instance, by using radial basis functions (e.g., Camus et al. 2011; Gouldby et al. 2014), kriging (Rohmer and Idier 2012), or genetic programming (Passarella et al. 2018). It should be noted that the quality of meta-models based on process-based simulations cannot be better than the used numerical model and thus introduce additional errors. Passarella et al. (2018) used a genetic programming approach to predict the total and infragravity swash excursion from observed data sets extensively used in swash prediction studies. One of the originalities of this work is that the final solutions are selected based on a minimization of the error while ensuring the formula could be interpreted physically and avoiding overfitting. While their approach reduces the prediction errors compared to well-established parameterization, as the one of Stockdon et al. (2006), it still depends on the learning dataset and the choice of the variables taken into account. The comparison (visual inspection) of the runup prediction of that study (Fig. 5 in Passarella et al. 2018) and the modelling results of Nicolae-Lerma et al. (2016, Fig. 4a therein) on the Truc Vert dataset show similar prediction quality. However, as highlighted by Passarella et al. (2018), even if the parameters they took into account (H_0, T_p, L_0, β) are easily accessible, they oversimplify the processes that affect swash. In addition, it is unknown how the predictors will perform in settings beyond those of their work, contrary to the kriging method which provides an error estimate.

4.2 Wave Contribution to Coastal Sea-Level Changes

In Sect. 2, we have shown how wave-induced processes could impact the sea level at the coast. These local processes are mostly controlled by offshore wave conditions, particularly the significant wave height and the wave period, which have been shown (Sect. 3) to vary significantly over decadal time scales, due to internal climate oscillations. Given the projected changes in atmospheric circulation induced by external forcing, it is likely that the wave climate will respond to these changes and adapt to the future wind regimes. The ensemble modeling of projected change in wave conditions realized during the COWCLIP project provides a global picture of the potential wave conditions for the end of the twenty-first century (see Fig. 7 and Sect. 3.4). Such changes will likely impact future coastal sea level. In addition, other interactions between waves and sea level need to be taken into account in order to understand the contribution of waves to coastal sea level. For instance, changes in water depth due to sea-level rise will relax the depth limitation of waves and could lead to higher and longer-period waves reaching the coast. These aspects are presented in this section.

Global-scale studies of coastal sea-level changes or flood-related risk assessments are often based on tide gauge records, which are mostly located in wave-sheltered areas. Yet,

regional- to global-scale studies accounting for wave contributions to past (e.g., Vous-doukas et al. 2016; Serafin et al. 2017; Rueda et al. 2017; Melet et al. 2018) and projected extreme sea levels (ESLs) at the coast are emerging (e.g., Vousdoukas et al. 2017, 2018a, b, Vitousek et al. 2017; Arns et al. 2017), although often assuming stationarity in the wave climate from past to future climate. These studies pinpoint the sizeable effects of wave contributions and the need to include them for coastal planning.

Vitousek et al. (2017) reported that when accounting for wave setup, wave runup, tides and storm surges, a sea-level rise of only 5–10 cm (expected to occur between 2030 and 2050) doubles the flooding frequency in many regions, particularly in the Tropics. Arns et al. (2017) reported that when accounting for wave contributions in future ESL, coastal protection design heights need to be increased by roughly 50% in the German Bight region relative to design heights inferred solely on sea-level rise. Focusing on future ESL along European coasts, Vousdoukas et al. (2017) showed that projected changes in storm surges and waves can substantially either enhance the effects of relative sea-level rise (along the majority of northern European coasts, locally with contributions up to 40%), or reduce it (along the Portuguese coast and the Gulf of Cadiz where reductions in surge and wave extremes offset relative sea-level rise by 20–30%). Global projections of ESL at the coast were recently provided by Vousdoukas et al. (2018a), accounting for wave setup. They reported a very likely increase in the globally averaged 100-year ESL of 34–76 cm under a moderate-emission-mitigation-policy scenario and of 58–172 cm under a business-as-usual scenario with wave setup being a non-dominant contributor to changes in extreme events. The important influence of changing wave contributions to coastal flooding due to increased water depth with sea-level rise was also reported in other studies (e.g., Hoeke et al. 2015; Wandres et al. 2017).

Wave setup and runup amplitude are modulated at longer timescales, notably through their dependence on offshore wave conditions. Wave height, period and direction vary
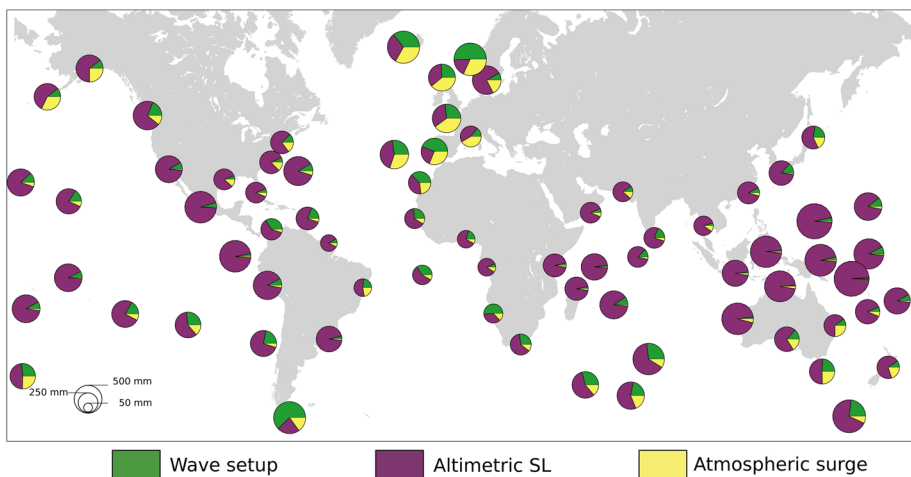
Fig. 10 Pie charts of the relative contribution of wave setup (green), altimetry-derived sea level (violet) and atmospheric surges (yellow) to total water-level detrended interannual-to-multidecadal variations over 1993–2015. The size of the pie charts indicates the standard deviation of detrended interannual-to-multidec-adal sea-level variations, with scalings on the lower left corner. Wave setup was estimated from the Stock-don et al. (2006) generic formulation with a spatially uniform shoreface slope of 0.05 and ERA-interim deep-water wave height and period. Adapted from Melet et al. (2018)

over a broad range of timescales, from seasonal to interannual and multidecadal scales in response to both internal climate variability (e.g., seasonality in storminess, climate modes of variability such as ENSO) and climate change (Sect. 3, see also Woodworth et al. 2019). Long-term changes in offshore wave conditions can therefore modulate wave energy fluxes and extreme water levels at the coast (e.g., Barnard et al. 2015; Mentaschi et al. 2017), and affect wave setup and swash at long timescales. Melet et al. (2016) reported a large contribution from wave runup to past changes in total coastal water level in the Gulf of Guinea at seasonal timescales. A first-order, quasi-global estimate of wave setup and swash contribution to interannual-to-decadal coastal water-level changes was recently provided by Melet et al. (2018), considering wave setup and runup changes induced only by changes in offshore wave height and period. Interannual-to-decadal wave setup changes were found to be significant in over large parts of the world coastline over the last two decades compared to other contributors to coastal sea-level changes (see Melet et al. 2018; and Fig. 10 herein). As reported by Serafin et al. (2017), who investigated the relative contribution of tides, waves and non-tidal residuals to extreme total water levels at the shoreline of US West Coast sandy beaches, regional differences in the magnitude of extreme total water levels can be attributed, in part, to changes in incident wave conditions through their contribution to the wave setup and wave runup. Therefore, the offshore regional wave climate variability presented in Sect. 3 may explain the regional differences in coastal sea-level changes reported by several authors (e.g., Melet et al. 2018; Vousdoukas et al. 2018a, b). For some regions, changes in the wave setup can substantially either enhance or attenuate the effect of thermal expansion and ice mass transfer from land-over periods of several decades. Melet et al. (2018) found that changes in the wave runup over the past two decades were mostly caused by internal climate variability.

It is important to stress that most of the aforementioned studies on the contribution of wave-induced processes to ESL and sea-level changes at global scale use empirical parameterizations with approximated inputs, which can hardly provide accurate estimates and sharp conclusions on the potential role of waves on global coastal water levels (see the comments from Aucan et al. 2019 and the associated response from Melet et al. Aucan et al. 2019; Melet et al. 2019). The most important limitations of these approaches are therefore discussed in a dedicated Sect. 5.4. However, all these studies converge to show that given the actual projections of future wave climate, it is likely that wave-induced processes will significantly impact future trends in coastal sea level, which need to be taken into account in future studies on regional sea-level change projections.

4.3 Interactions with Other MSL-Related Processes

Several interactions between waves and lower-frequency sea-level components can be identified, among which are: (1) the effect of water depth modulation and currents on waves and (2) the effect of waves on atmospheric storm surge. Here, we introduce studies providing quantifications of these effects, mainly based on Idier et al. (2019), who also detail the related mechanisms.

In the nearshore, tides can significantly modify short waves. First, tide-induced water-level variations shift the cross-shore position of the surf zone, so that wave heights are modulated along a tidal cycle (e.g., Dodet et al. 2013). In addition, strong tidal currents (as in straits, estuaries or tidal inlets) can affect the waves (Rusu et al. 2011). As a consequence, wave setup along the shoreline or inside estuary can exhibit tidal modulations with a wave setup being smaller at high tide than at low tide (see, e.g., Kim et al. 2008), or

the opposite (Dodet et al. 2018), depending on the curvature of the foreshore slope. At a given location, modulations of several centimeters to tens centimeters have been estimated in many studies, both in estuaries (see, e.g., Fortunato et al. 2017; Tagus estuary, Portugal) or on wave-dominated beaches (see, e.g., Pedreros et al. 2018; Truc Vert Beach, France). As an additional mechanism, we should note that, in estuaries, the wave setup can be also amplified through a resonant process (Fortunato et al. 2017).

Several studies investigated the effect of SLR on waves, taking into account tide changes or tide and atmospheric storm surges changes (see, e.g., Chini et al. 2010; Arns et al. 2017). In the German Bight, at the exposed westward-oriented coast, the modeling results of Arns et al. (2017) show that the significant wave height of the most damaging combination (still water level, wave height) of probability 0.01/year would exceed the present conditions by up to 0.25 m (0.78 m), for SLR = 0.54 m (1.74 m). They also show that with the sea-level rise, at a given location, the tide-induced modulation of waves decreases (see, e.g., Arns et al. 2017). However, the absolute results of these studies should be used with caution as the bathymetry is generally assumed unchanged (which is a strong assumption considering that sea-level rise should have significant effect).

Waves and wave setup are modified by water depth and currents, but they also have an effect on atmospheric storm surges, as the surface stress also depends on the sea state, through the sea-surface roughness (see, e.g., Stewart et al. 2013). These modifications of sea-surface roughness by waves can lead to atmospheric surge amplification up to tens of centimeters. For instance, Bertin et al. (2012) investigated the wave-induced processes explaining the large storm surge in the Bay of Biscay associated with the Xynthia storm in February 2010. They compared the atmospheric surges obtained with quadratic formulation to the ones obtained with wave-dependent parameterization to compute wind stress and they found that both approaches performed similarly except during the storm peak, where the surge with the wave-dependent parameterization was several tens of centimeters larger. Similar order of magnitudes is obtained, for instance, in the North Sea (Mastenbroek et al. 1993) or the Taiwan Strait (Zhang et al. 2010).

In coastal zones, the near-bottom orbital velocities associated with the propagation of short waves can become large and enhance bottom stress (Grant and Madsen 1986), including the formation of ripples (Ardhuin et al. 2002a, b). This enhancement should reduce the storm surges. However, this effect remains to be validated with field measurements in shallow water.

5 Limitation and Perspectives

5.1 Measurements of Waves

With seven altimeters in operations as of September 2018 (Fig. 4a), offshore wave heights are better monitored than ever, and higher along-track resolution is now available thanks to improved retracking and filtering. Because wave-induced sea level at the coast is a function of the wave periods (e.g., Stockdon et al. 2006; Poate et al. 2016; Dodet et al. 2018) and directional wave properties (Guza and Feddersen 2012), the availability of spectral wave information is critical. For large ocean basins, and in particular in the Pacific, SAR-derived swell measurements, such as from Sentinel-1, is a very rich source of data. Extending such measurements to shorter wave periods will allow the monitoring of wave periods
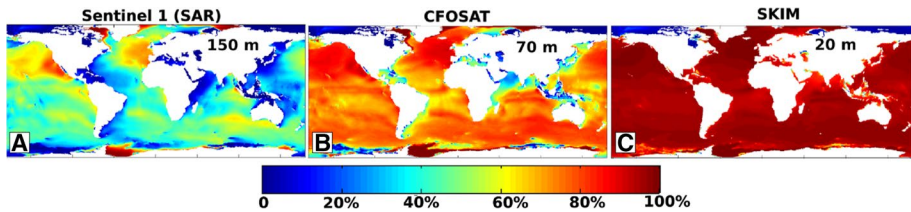
Fig. 11 Average fraction of simulated wave energy in January 2014 resolved when using a cutoff wavelength of 150 m (**a**), 70 m (**b**) and 20 m (**c**). Note that low values in the Arctic and other ice-covered regions are an artifact of the model that does not properly represent wave–ice interactions. January 2014 was very stormy in the North Atlantic

and directions in and near storms and in smaller basins. Indeed, the main limitation of SARs is due to the blurring associated with orbital velocities (Alpers and Rufenach 1979), which limits the effective resolution of waves that propagate in the satellite flight direction. This blurring is proportional to the altitude of the satellite. As a result, conditions are generally not satisfactory for measuring waves with SARs in enclosed basins or off eastern coasts (Fig. 11a). This is the main motivation for the development of specific "wave spectrometers," based on a conically scanning real aperture radars (RARs, see Jackson et al. 1985; Hauser et al. 2017; Nouguier et al. 2018). The first satellite to carry such a Ku-band RAR instrument is CFOSAT, successfully launched on October 29, 2018. This instrument is expected to resolve waves as short as 70 m, with a 180° ambiguity on the wave propagation direction (Fig. 11b). The next generation of such an instrument is ESA's Sea surface KInematics Multiscale (SKIM) monitoring mission, resolving much shorter wavelengths without direction ambiguity thanks to a Doppler measurement, and this could be launched in 2025 (Ardhuin et al. 2018). Such a resolution would allow the measurement of dominant waves in all seas, with a typical revisit time of 4 days (Fig. 11c).

All these wave measurements fail very close to the shore (50 km for altimeters, a few meters for SARs with a strong perturbation by the surf zone) and are typically used for validating the offshore part of numerical wave models that simulate waves up to the coast. However, recent developments in processing (e.g., Passaro et al. 2015; Ardhuin et al. 2017) or filtering techniques (Quilfen et al. 2018) enable data to be used at much higher resolution, possibly down to 20 km, whereas standard wave heights from altimeters (e.g., Sepulveda et al. 2015) are typically dominated by noise for scales shorter than 50 km.

Concerning our understanding of the complex wave deformation in the surf zone, new insights have been obtained with LiDAR scanners deployed along a pier at Saltburn beach, UK (Martins et al. 2017). This technique provides measurements of the sea-surface elevation from the break point to the runup limit at spatial (centimeters) and temporal (25 Hz) resolutions rarely achieved in field conditions. Such innovative measurements will undoubtedly foster our understanding of depth-limited wave-breaking mechanism and swash zone hydrodynamics and improve the accuracy of parametric formula used to infer nearshore parameters from deep-water wave measurements.

The modelling of waves right up to the coast requires a good knowledge of nearshore depths and currents that is missing in many regions. With some progress coming from the exceptional coverage of new optical sensors mounted on board of satellites such as Sentinel 2, both radiance-based methods (e.g., Purkis 2018) and new methods based on dispersion (e.g., Kudryavtsev et al. 2017; Romeiser and Graber 2018) will certainly lead to rapid progress on this topic. In addition, altimeter data can be efficiently used to apply directional

correction to modeled wind sea and swell wave height, as demonstrated by Albuquerque et al. (2018).

Finally, the satellite remote sensing of a sea level that include wave effects, right at the coast, has not yet been demonstrated. Today's nadir altimeters only provide offshore sea levels, and it is unclear how much the noise in future measurements of SWOT's across-track SAR interferometer (Durand et al. 2010) may corrupt data across the surf zone, with additional velocity bunching and azimuthal cutoff effects.

5.2 Coastal Bathymetry

Recent studies have shown that extreme winter wave conditions can have a dramatic impact on beach morphologies at regional scale and over pluri-annual time periods (Masselink et al. 2016; Dodet et al. 2019). Therefore, it seems over-simplistic to consider that coastal vulnerability (shoreline retreat and flooding) can be represented as a simple response to sea-level change, assuming passive coastal bathymetry. Although constant efforts by the research community have been made toward either simple or complex paradigms of coastal evolution (e.g., static retreat by Bruun 1962), the coastal response to perpetually changing ocean-forcing conditions is still unclear (Cooper and Pilkey 2004; Ranasinghe 2016). Recently, several methods using satellite imagery have been proven reliable (Poupardin et al. 2016; Bergsma et al. 2019; Almar et al. 2019; Raucoules et al. 2019) in estimating large-sale coastal bathymetry at unprecedented resolution. One prominent approach is the use of multispectral imagery in estimating shallow bathymetry, until 20 m depth approximately in the case of clear waters. However, many coastal waters are very turbid, and this method requires ground-based calibration, which limits this technique to accessible areas. Other techniques to estimate bathymetry from optical or radar imagery make use of the wavelengths change during the shoaling of ocean waves. This allows resolving depths up to 40–50 m in regions where long swells are present. Among these methods, some use external data (measurements or offshore modeling), while others directly extract the wavelength and wave celerity information from the satellite images. Despite their high potential, these methods were only applied to a limited spatial domain (Danilo and Melgani 2016; Poupardin et al. 2016) using basic wave physics (none uses the information contained in the full spectrum in an optimal way) and can still be improved. Having access to high-resolution coastal bathymetry is one major prerequisite in order to reduce uncertainty in the estimation of wave contribution to coastal sea-level changes (e.g., Melet et al. 2018), and the aforementioned studies appear as promising avenue to tackle this challenge.

5.3 Stochastic Character of Wind-Generated Waves

Our ability to predict wave overtopping is crucial for coastal management. It should be reminded that an infinite number of time series could occur for a same-wave spectrum (Tuah and Hudspeth 1982). Pearson et al. (2001) raised the issue of the relationship between the length of the time series and the accuracy of the overtopping estimate. Pullen et al. (2007) recommend simulating a sequence of 1000 waves for each sea state tested. Pearson et al. (2001) and Romano et al. (2015) noticed that the overtopping discharge from tests using series of 500 waves is very close to that from tests with 1000 waves, while Williams et al. (2014) show that using more than 1000 waves does not affect the overtopping estimate. This suggests that the effect of stochastic character of waves on overtopping

discharge depends on the time span during which the parameters influencing the waves are almost constant. Considering a wave period of 12 s, the time span should be larger than 1h40 min. In micro-tidal environment, such conditions could be met. However, in macrotidal environments, as highlighted in Sect. 4.3, nearshore waves are modulated by tides, and water level can exhibit changes up to a few meters in a single hour. This implies that the stochastic character of waves should have a significant effect on flood occurrence or overtopping discharge, especially in macro-tidal environment. This subject should deserve more attention in the future.

5.4 Empirical Formulations for Wave Setup and Runup

While wave setup and runup derived from empirical formulations can compare well to observations when local characteristics of the coast are available (e.g., Vousdoukas et al. 2009; Stockdon et al. 2006), this approach can lead to uncertain results at global scales for several reasons: First, generic formulations of wave setup and runup involve the foreshore slope, which vary significantly in space and time (e.g., Hoeke et al. 2015; Karunarathna et al. 2016; Díez et al. 2017), and are usually within the 1–20% range (e.g., Komar 1998; Defeo and McLachlan 2013). Yet, as foreshore beach slopes are unknown over most of the world coastlines, regional- to global-scale studies have used constant values of the foreshore beach slope (e.g., Melet et al. 2018; Serafin et al. 2017), constant values of sediment grain size to infer beach slopes (Rueda et al. 2017), or formulations specific to dissipative beaches that do not depend on the beach slope (e.g., Vitousek et al. 2017). Wave setup estimates are very sensitive to the beach slope value and to the chosen empirical formulation, so that reported wave setup contributions are therefore to be modulated by the local beach slope compared to estimates using a uniform spatial value. It should also be noted that accounting for the variability of the beach slope should modulate the spatial heterogeneity of wave setup changes. Second, the widely used empirical formulation of Stockdon et al. (2006) for wave setup and runup has been derived from field observations on sandy beaches and does not encompass the variety of coastal environments that can be found worldwide (gravel beaches, cliffs, armored coasts, etc). It is therefore important to test and derive new empirical formula for other types of environment. In addition, deep-water wave characteristics derived from global numerical models to estimate wave setup and runup from empirical formulations also come with limitations. In particular for extreme events, storm winds tend to be underestimated in global simulations (especially for tropical cyclones). Finally, global-scale studies of coastal sea-level changes including the contribution from wave setup or runup do not account for interactions between the different contributors to sea-level changes (e.g., tides, waves, surges, ocean circulation, SLR) as global-scale numerical modeling studies including all the aforementioned processes are not available yet.

5.5 Projections from General Circulation Models

Predicting how wave-induced processes will contribute to future coastal sea-level changes requires accurate information on future wave conditions. For this purpose, general circulation models integrate the major physical processes of the atmosphere, ocean, cryosphere and land surface in order to simulate the response of the global climate system to increasing greenhouse gas concentrations. Although GCMs are extremely valuable tools to estimate the magnitude and trends of essential climate variables in the near future, their results

are flawed by cumulative uncertainties inherent to each layer that constitutes these complex modeling systems (e.g., expected accumulation of greenhouse gases and aerosols in the atmosphere, response of the atmospheric circulation, interactions with the hydrosphere, cryosphere, lithosphere and biosphere, global-to-regional downscaling). Concerning ocean waves, the main driver is the atmospheric circulation and more particularly the 10-m wind fields that are usually used to force numerical wave models. As stated in the 5th Annual Report of the IPCC (chapter 13, Church et al. 2013), there is *low confidence* in global wave model projections because of uncertainties regarding future wind states, particularly storm geography, the limited number of model simulations used in the ensemble averages, and the different methodologies used to downscale climate model results to regional scales (Hemer et al. 2013b). In a recent paper, Morim et al. (2018) analyze 91 published global and regional wave climate projection studies and found a lack of consensus for projections of H_s over the eastern North Pacific and southern Indian and Atlantic Oceans, and everywhere, except for the Southern Ocean and the North Atlantic, for extreme H_s. They also note a distinct lack of research regarding projected changes in wave direction, which is of critical importance for the impact of waves on coastal sea level. Finally, they recommend a shift toward a systematic, community-based framework (as proposed by the Coordinated Ocean Wave Climate Project—COWCLIP, Hemer et al. 2018) to foster concerted efforts and to better inform the wide range of relevant decisions across ocean and coastal adaptation and mitigation assessments.

6 Conclusion

We have seen that the coastal sea level, as observed at the shores of exposed coastlines, is strongly influenced by wave-induced processes. Despite its central importance for risk mitigation and sustainable management of the coastal zone, the coastal sea level has for long been assimilated to the sea level estimated from tidal gauges located in sheltered areas, where the effect of the waves is limited. In addition, the rich information on global sea-level variability recorded by satellite altimeters over the last 30 years cannot be extrapolated to the coast where the presence of lands degrades altimeter echoes. As a consequence, our understanding of the regional and long-term variability of coastal sea level, and particularly its wave-related components, is still very limited. We claim in this paper that this topic deserves much attention. The three major wave-related processes that affect coastal sea level are (1) the wave setup: a tilt of the water surface in the surf zone caused by the rapid dissipation of wave energy at the breaking point; (2) the wave runup: the vertical excursion of the waterline when the waves enter the swash zone; (3) the infragravity waves: low-frequency (~ 0.01 Hz) oscillations of the water surface bound to and travelling with the wave groups that increase in size in the shoaling and breaking zone and significantly contribute to the swash motions. All these processes are controlled by offshore wave parameters, such as the significant wave height, the wave period and the wave direction. Given the strong variabilities (seasonal, interannual, decadal) of incident offshore wave conditions, the contribution of wave-related components is known to impact coastal sea level over a wide range of scales. Moreover, a number of studies on past and future trends in wave conditions indicate that significant changes in the height, direction and periods of wind-generated waves are imprinted by internal and external climate variabilities. These long-term changes in wave conditions will likely affect coastal sea level, and preliminary assessments of the wave-related contribution to coastal sea level have already confirmed

this idea. However, severe limitations still restrain a clear understanding about the role of waves on coastal sea-level variability. These limitations concern: the lack of satellite information at the coast and on the wave period and direction, the difficulty to obtain accurate bathymetric information in the nearshore, where bottom features are constantly evolving, the high computational cost of high-resolution model needed to resolve the complex wave transformation from deep water to the shore, the overly simplistic form of empirical models used to derive wave setup and runup from offshore wave parameters, and the large uncertainties associated with future projections of wind and wave conditions at regional scales. Fortunately, great advances are currently shaping the fields of remote sensing observations, geophysical data analysis, and high-level computer science, which will pave the way for a deeper understanding of the contribution of wind-generated waves to coastal sea level.

References

Abessolo Ondoa G, Almar R, Castelle B, Testut L, Leger F, Bonou F, Bergsma E, Meyssignac B, and Larson M (2019) On the use of shore-based video camera to monitor sea level at the coast: A case study in grand popo, benin (Gulf of Guinea, West Africa). J Atmos Ocean Technol (in review)

Albuquerque J, Antolínez JAA, Rueda A, Méndez FJ, Coco G (2018) Directional correction of modeled sea and swell wave heights using satellite altimeter data. Ocean Model 131:103–114. https://doi.org/10.1016/j.ocemod.2018.09.001

Allender J, Audunson T, Barstow SF, Bjerken S, Krogstad HE, Steinbakke P, Vardtal L, Borgman LE, Graham C (1989) The WADIC project: a comprehensive field evaluation of directional wave instrumentation. Ocean Eng 16:505–536

Almar R, Blenkinsopp C, Almeida LP, Cienfuegos R, Catalan P (2017) Wave runup video motion detection using the Radon Transform. Coast Eng 130:46–51

Almar R, Bergsma EWJ, Maisongrande P, Melo de Almeida LP (2019) Wave-derived coastal bathymetry from satellite video imagery: a showcase with Pleiades persistent mode. Remote Sens Environ. https://doi.org/10.1016/j.rse.2019.111263

Almeida LP, Masselink G, Russell PE, Davidson MA (2015) Observations of gravel beach dynamics during high energy wave conditions using a laser scanner. Geomorphology 228:15–27. https://doi.org/10.1016/j.geomorph.2014.08.019

Almeida LP, Almar R, Meyssignac B, Viet NT (2018) Contributions to coastal flooding events in southeast of Vietnam and their link with global mean sea level rise. Geosciences 8:437

Alpers W, Rufenach C (1979) The effect of orbital motions on synthetic aperture radar imagery of ocean waves. IEEE Trans Antennas Propag 27:685–690. https://doi.org/10.1109/TAP1979.1142163

Aouf L, Lefèvre JM, Hauser D, Chapron B (2006) On the combined assimilation of RA-2 altimeter and ASAR wave data for the improvement of wave forecasting. In: Proceedings of 15 years of radar altimetry symposium, Venice, March 13–18, 2006

Apotsos A, Raubenheimer B, Elgar S, Guza R, Smith JA (2007) Effects of wave rollers and bottom stress on wave setup. J Geophys Res Oceans 112(C2):C02003

Ardhuin F, Orfila A (2018) Wind waves. New Front Oper Oceanog 14:393–422. https://doi.org/10.17125/gov2018.ch14

Ardhuin F, Drake TG, Herbers THC (2002a) Observations of wave-generated vortex ripples on the North Carolina continental shelf. J Geophys Res Oceans 107:7-1–7-14. https://doi.org/10.1029/2001JC000986

Ardhuin F, Drake TG, Herbers THC (2002b) Observations of wave-generated vortex ripples on the North Carolina continental shelf. J Geophys Res 107:C10. https://doi.org/10.1029/2001JC000986

Ardhuin F, Herbers THC, Jessen PF, O'Reilly WC (2003) Swell transformation across the continental shelf. Part II: validation of a spectral energy balance equation. J Phys Oceanogr 33:1940–1953

Ardhuin F, Rascle N, Belibassakis KA (2008a) Explicit wave-averaged primitive equations using a generalized Lagrangian mean. Ocean Model 20(1):35–60

Ardhuin F, Jenkins AD, Belibassakis KA (2008b) Comments on the three-dimensional current and surface wave equations. J Phys Oceanogr 38(6):1340–1350

Ardhuin F, Rascle N, Belibassakis KA (2008c) Explicit wave-averaged primitive equations using a generalized Lagrangian mean. Ocean Model 20:35–60. https://doi.org/10.1016/j.ocemod.2007.07.001

Ardhuin F, Rascle N, Chapron B, Gula J, Molemaker J, Gille ST, Menemenlis D, Rocha C (2017) Small scale currents have large effects on wind wave heights. J Geophys Res 122(C6):4500–4517. https://doi.org/10.1002/2016JC012413

Ardhuin F, Aksenov Y, Benetazzo A, Bertino L, Brandt P, Caubet E, Chapron B, Collard F, Cravatte S et al (2018) Measuring currents, ice drift, and waves from space: the Sea surface KInematics Multiscale monitoring (SKIM) concept. Ocean Sci 14:337–354. https://doi.org/10.5194/os-2017-65

Ardhuin F, Stopa JE, Chapron B, Collard F, Husson R, Jensen RE, Johannessen J, Mouche A, Passaro M,Quartly GD, Swail V, Young I (2019) Observing sea states. Front Mar Sci. https://doi.org/10.3389/fmars.2019.00124

Arns A, Wahl T, Dangendorf S, Jensen J, Pattiaratchi C (2017) Sea-level rise induced amplification of coastal protection design heights. Nat Sci Rep. https://doi.org/10.1038/srep40171

Atkinson AL, Power HE, Moura T, Hammond T, Callaghan DP, Baldock TE (2017) Assessment of runup predictions by empirical models on non-truncated beaches on the south-east Australian coast. Coast Eng 119:15–31

Aucan J, Hoeke RK, Storlazzi CD, Stopa J, Wandres M, Lowe R (2019) Waves do not contribute to global sea-level rise. Nat Clim Change 9:2. https://doi.org/10.1038/s41558-018-0377-5

Barber NF, Ursell F, Darbyshire J, Tucker MJ (1946) A frequency analyser used in the study of ocean waves. Nature 158:329–335

Barnard PL, Short AD, Harley MD, Splinter KD, Vitousek S, Turner IL, Allan J, Banno M, Bryan KR, Doria A, Hansen JE, Kato S, Kuriyama Y, Randall-Goodwin E, Ruggiero P, Walker IJ, Heathfield DK (2015) Coastal vulnerability across the Pacific dominated by El Niño/Southern Oscillation. Nat Geosci 8:801–807. https://doi.org/10.1038/ngeo2539

Battjes JA (1974) Surf similarity. In: Proceedings of the 14th conference of Coast Eng. ASCE, 466–48

Battjes JA, Bakkenes HJ, Janssen TT, van Dongeren AR (2004) Shoaling of subharmonic gravity waves. J Geophys Res 109:c02009. https://doi.org/10.1029/2003JC001863

Bennis AC, Dumas F, Ardhuin F, Blanke B (2014) Mixing parameterization: impacts on rip currents and wave set-up. Ocean Eng 84:213–227

Bergsma EWJ, Almar R (2018) Video-based depth inversion techniques, a method comparison with synthetic cases. Coast Eng 138:199–209

Bergsma EWJ, Almar R and Maisongrande P (2019) Radon-augmented SentinelII satellite imagery to derive wave-patterns and regional bathymetry. IEEE Trans Geosci Remote Sens (in review)

Bertin X, Bruneau N, Breilh JF, Fortunato AB, Karpytchev M (2012) Importance of wave age and resonance in storm surges: the case Xynthia, Bay of Biscay. Ocean Model 42:16–30. https://doi.org/10.1016/j.ocemod.2011.11.001

Bertin X, Prouteau E, Letetrel C (2013) A significant increase in wave height in the North Atlantic Ocean over the 20th century. Glob Planet Change. https://doi.org/10.1016/j.gloplacha.2013.03.009

Bertin X, Li K, Roland A, Bidlot JR (2015) The contribution of short-waves in storm surges: two case studies in the Bay of Biscay. Cont Shelf Res 96:1–15

Bertin X, Olabarrieta M, MacCall R (2017) Hydrodynamics under storm conditions. In: Coastal storms: processes and impacts. Wiley, London

Bertin X, de Bakker A, van Dongeren A, Coco G, André G, Ardhuin F, Bonneton P, Bouchette F, Castelle B, Crawford WC, Davidson M, Deen M, Dodet G, Guérin T, Inch K, Leckler F, McCall R, Muller H, Olabarrieta M, Roelvink D, Ruessink G, Sous D, Stutzmann E, Tissier M (2018) Infragravity waves: from driving mechanisms to impacts. Earth Sci Rev 177:774–799. https://doi.org/10.1016/j.earscirev.2018.01.002

Bidlot JR (2017) Intercomparison of operational wave forecasting systems against buoys: data from ECMWF, MetOffice, FNMOC, ECCC, NCEP, MeteoFrance, DWD, BoM, SHOM, JMA, KMA, Puerto del Estado, DMI, NZM, METNO, SHN-SM, September 2017 to November 2017, tech. rep, Joint WMO-IOC Technical Commission for Oceanography and Marine Meteorology, 2017

Biesel F (1952) Équations générales au second ordre de la houle irrégulière. La Houille Blanche 7(3):372–376. https://doi.org/10.1051/lhb/1952033

Birkemeier WA (1997) The sandyduck '97 nearshore field experiment. Defense Technical Information Center, Fort Belvoir. https://doi.org/10.21236/ADA629329

Blenkinsopp CE, Mole MA, Turner IL, Peirson WL (2010) Measurements of the time-varying free-surface profile across the swash zone obtained using an industrial LIDAR. Coast Eng 57:1059–1065. https://doi.org/10.1016/j.coastaleng.2010.07.001

Bonneton P, Barthelemy E, Chazel F, Cienfuegos R, Lannes D, Marche F, Tissier M (2011) Recent advances in Serre-Green Naghdi modelling for wave transformation, breaking and runup processes. Eur J Mech B Fluids 30:589–597

Bonneton A, Lannes D, Martins K, Michallet H (2017) Nonlinear weakly dispersive method for recovering the elevation of irrotational surface waves from pressure measurements. Coast Eng. https://doi.org/10.1016/j.coastaleng.2018.04.005

Bowen AJ (1969) Rip currents. Theoretical investigations. J Geophys Res 74:5467–5478

Bowen AJ, Guza R (1978) Edge waves and surf beat. J Geophys Res 83:1913–1920

Bowen AJ, Inman DL, Simmons VP (1968) Wave 'set-down' and set-Up. J Geophys Res 73:2569–2577. https://doi.org/10.1029/JB073i008p02569

Brodie KL, Raubenheimer B, Elgar S, Slocum RK, McNinch JE (2015) Lidar and pressure measurements of inner-surfzone waves and setup. J Atmos Ocean Technol 32:1945–1959. https://doi.org/10.1175/JTECH-D-14-00222.1

Brodie KL, Palmsten ML, Hesser TJ, Dickhudt PJ, Raubenheimer B, Ladner H, Elgar S (2018) Evaluation of video-based linear depth inversion performance and applications using altimeters and hydrographic surveys in a wide range of environmental conditions. Coast Eng 136:147–160

Bromirski PD, Cayan DR, Flick RE (2005) Wave spectral energy variability in the northeast Pacific. J Geophys Res 110:C03005. https://doi.org/10.1029/2004JC002398

Bromirski PD, Cayan DR, Helly J, Wittmann P (2013) Wave power variability and trends across the North Pacific. J Geophys Res Oceans 118:6329–6348. https://doi.org/10.1002/2013JC009189

Bruneau N, Fortunato AB, Dodet G, Freire P, Oliveira A, Bertin X (2011) Future evolution of a tidal inlet due to changes in wave climate, Sea level and lagoon morphology (Óbidos lagoon, Portugal). Cont Shelf Res 31:1915–1930. https://doi.org/10.1016/j.csr.2011.09.001

Bruun P (1962) Sea-level rise as a cause of shore erosion. J Waterw Har Div 88:117–132

Camus P, Mendez FJ, Medina R (2011) A hybrid efficient method to downscale wave climate to coastal areas. Coast Eng 58:851–862. https://doi.org/10.1016/j.coastaleng.2011.05.007

Camus P, Mendez FJ, Losada I, Menendez M, Espejo A, Pérez J, Rueda A, Guanche Y (2014a) A method for finding the optimal predictor indices for local wave climate conditions. Ocean Dyn 64:1025–1038. https://doi.org/10.1007/s10236-014-0737-2

Camus P, Menendez M, Mendez FJ, Izaguirre C, Espejo A, Canovas V, Perez J, Rueda A, Losada IJ, Medina R (2014b) A weather-type statistical downscaling framework for ocean wave climate. J Geophys Res Oceans 119:7389–7405. https://doi.org/10.1002/2014jc010141

Camus P, Losada IJ, Izaguirre C, Espejo A, Menéndez M, Pérez J (2017) Statistical wave climate projections for coastal impact assessments. Earth's Future 5:918–933. https://doi.org/10.1002/2017EF000609

Carrier GF, Greenspan HP (1958) Water waves of finite amplitude on a sloping beach. J Fluid Mech 4:97–109. https://doi.org/10.1017/S0022112058000331

Carter DJT, Draper L (1988) Has the north-east Atlantic become rougher? Nature 332:494–494. https://doi.org/10.1038/332494a0

Casas-Prat M, Wang XL, Swart N (2018) CMIP5-based global wave climate projections including the entire Arctic Ocean. Ocean Model 123:66–85. https://doi.org/10.1016/j.ocemod.2017.12.003

Castelle B, Marieu V, Bujan S, Ferreira S, Parisot J.-P, Capo S, Sénéchal N, Chouzenoux T (2014) Equilibrium shoreline modelling of a highenergy meso-macrotidal multiple-barred beach. Mar Geol 347:85–94. https://doi.org/10.1016/j.margeo.2013.11.003

Castelle B, Dodet G, Masselink G, Scott T (2018) Increased winter-mean wave height, variability, and periodicity in the Northeast Atlantic over 1949–2017. Geophys Res Lett 45:3586–3596. https://doi.org/10.1002/2017GL076884

Cazenave A, Cozannet GL (2014) Sea level rise and its coastal impacts. Earth's Future 2:15–34. https://doi.org/10.1002/2013EF000188

Cazenave et al (WCRP Global Sea Level Budget Group) (2018) Global sea-level budget 1993–present. Earth Syst Sci Data 10:1551–1590. https://doi.org/10.5194/essd-10-1551-2018

Charles E, Idier D, Thiébot J, Le Cozannet G, Pedreros R, Ardhuin A, Planton S (2012) Present wave climate in the Bay of Biscay: spatiotemporal variability and trends from 1958 to 2001. J Climate 25:2020–2039. https://doi.org/10.1175/JCLI-D-11-00086.1

Chen Q, Kirby JT, Dalrymple RA, Shi F, Thornton EB (2002) Boussinesq modeling of longshore currents. J Geophys Res 108(C11):3362. https://doi.org/10.1029/2002jc001308

Cheriton OM, Storlazzi CD, Rosenberger KJ (2016) Observations of wave transformation over a fringing coral reef and the importance of low-frequency waves and offshore water levels to runup, overwash, and coastal flooding. J Geophys Res Oceans 121(5):3121–3140

Chini N, Stansby P, Leake J, Wolf J, Roberts-Jones J, Lowe J (2010) The impact of sea level rise and climate change on inshore wave climate: a case study for East Anglia (UK). Coast Eng 57(11–12):973–984. https://doi.org/10.1016/j.coastaleng.2010.05.009

Church JA, Clark PU, Cazenave A, Gregory JM, Jevrejeva S, Levermann A, Merrifield MA, Milne GA, Nerem RS, Nunn PD, Payne AJ, Pfeffer WT, Stammer D, Unnikrishnan AS (2013) Sea level change. In: Stocker TF, Qin D, Plattner G.-K, Tignor M, Allen SK, Boschung J, Nauels A, Xia Y, Bex V, Midgley PM (eds) Climate change 2013: the physical science basis. Contribution of working group I to the fifth assessment report of the intergovernmental panel on climate change. Cambridge University Press, Cambridge, pp 1137–1216. https://doi.org/10.1017/CBO9781107415324.026

Cipollini P, Benveniste J, Birol F, Joana Fernandes M, Obligis E, Passaro M, Ted Strub P, Valladeau G, Vignudelli S, Wilkin J (2017) Satellite altimetry in coastal regions. In: Satellite altimetry over oceans and land surfaces, pp 343–380. https://doi.org/10.1201/9781315151779

Cohn N, Ruggiero P (2016) The influence of seasonal to interannual nearshore profile variability on extreme water levels: modeling wave runup on dissipative beaches. Coast Eng 115:79–92

Cooper JAG, Pilkey OH (2004) Sea-level rise and shoreline retreat: time to abandon the Bruun Rule. Glob Planet Change 43:157–171. https://doi.org/10.1016/j.gloplacha.2004.07.001

Crawford W, Ballu V, Bertin X, Karpytchev M (2015) The sources of deep ocean infragravity waves observed in the North Atlantic Ocean. J Geophys Res 120:5120–5133. https://doi.org/10.1002/2014JC010657

Crosby SC, Cornuelle BD, O'Reilly WC, Guza RT (2017) Assimilating global wave model predictions and deep-water wave observations in nearshore swell predictions. J Atmos. Ocean Technol 34:1823–1836. https://doi.org/10.1175/JTECH-D-17-0003.1

Danilo C, Melgani F (2016) Wave period and coastal bathymetry using wave propagation on optical images. IEEE Trans Geosci Remote Sens 54:6307–6319. https://doi.org/10.1109/TGRS2016.2579266

De Bakker ATM, Tissier MFS, Ruessink BG (2014) Shoreline dissipation of infragravity waves. Cont Shelf Res 72:73–82. https://doi.org/10.1016/j.csr.2013.11.013

Dean RG (1977) Equilibrium beach profiles: U.S. atlantic and gulf coasts. Department of Civil Engineering and College of Marine Studies, University of Delaware

Di Luccio D, Benassai G, Budillon G, Mucerino L, Montella R, Pugliese Carratelli E (2018) Wave run-up prediction and observation in a micro-tidal beach. Nat Hazards Earth Syst Sci 18:2841–2857

Díaz-Sánchez R, López-Gutiérrez JS, Lechuga A, Negro V (2014) Runup variability due to time dependence and stochasticity in the beach profiles: two extreme cases of the Spanish coast. J Coast Res 70:1–6. https://doi.org/10.2112/SI70-001.1

Díez J, Uriarte A, Cánovas V, Medina R (2017) A parametric model for dry beach equilibrium profiles. Coast Eng 127:134–144

Dodet G, Bertin X, Taborda R (2010) Wave climate variability in the North-East Atlantic Ocean over the last six decades. Ocean Model 31:120–131. https://doi.org/10.1016/j.ocemod.2009.10.010

Dodet G, Bertin X, Bruneau N, Fortunato A, Nahon A, Roland A (2013) Wave-current interactions in a wave-dominated tidal inlet. J Geophys Res Ocean 118:1587–1905. https://doi.org/10.1002/jgrc.20146

Dodet G, Leckler F, Sous D, Ardhuin F, Filipot JF, Suanez S (2018) Wave runup over steep rocky cliffs. J Geophys Res Oceans 123:7185–7205. https://doi.org/10.1029/2018JC013967

Dodet G, Castelle B, Masselink G, Scott T, Davidson M, Floc'h F, Jackson D, Suanez S (2019) Beach recovery from extreme storm activity during the 2013/14 winter along the Atlantic coast of Europe. Earth Surf Process Landf. https://doi.org/10.1002/esp.4500

Durand M, Fu L, Lettenmaier DP, Alsdorf DE, Rodriguez E, Esteban-Fernandez D (2010) The surface water and ocean topography mission: Observing terrestrial surface water and oceanic submesoscale eddies. Proc IEEE 98:766–779. https://doi.org/10.1109/JPROC.2010.2043031

Elgar S, Herbers THC, Okihiro M, Oltman-Shay J, Guza RT (1992) Observations of infragravity waves. J Geophys Res Oceans 97:15573–15577. https://doi.org/10.1029/92JC01316

Fiedler JW, Brodie KL, McNinch JE, Guza RT (2015) Observations of runup and energy flux on a low-slope beach with high-energy, long-period ocean swell. Geophys Res Lett. https://doi.org/10.1002/2015gl066,124

Ford M, Merrifield MA, Becker JM (2018) Inundation of a low-lying urban atoll island: Majuro, Marshall Islands. Nat Hazards 91(3):1273–1297. https://doi.org/10.1007/s11069-018-3183-5

Fortunato AB, Freire P, Bertin X, Rodrigues M, Liberato MLR, Ferreira J (2017) A numerical study of the February 15, 1941 storm in the Tagus estuary. Cont Shelf Res 144:50–64. https://doi.org/10.1016/j.csr.2017.06.023

Gain L (1923) La prédiction des houles au Maroc. Revue Scientifique 61(19):605–615

Gainza J, Rueda A, Camus P, Tomas A, Méndez FJ, Sano M, and Tomlinson R (2018) A meta-modelling approach for estimating long-term wave run-up and total water level on beaches. J Coast Res 34(2):475–489. Coconut Creek (Florida), ISSN 0749-0208

Garcez-Faria A, Thornton E, Lippmann T, Stanton T (2000) Undertow over a barred beach. J Geophys Res Oceans 105(C7):16999–17010

Gawehn M, van Dongeren A, van Rooijen A, Storlazzi CD, Cheriton OM, Reniers A (2016) Identification and classification of very low frequency waves on a coral reef flat. J Geophys Res Oceans 121(10):7560–7574

Gemmrich J, Thomas B, Bouchard R (2011) Observational changes and trends in northeast Pacific wave records. Geophys Res Lett. https://doi.org/10.1029/2011GL049518

Gouldby B, Méndez FJ, Guanche Y, Rueda A, Mínguez R (2014) A methodology for deriving extreme nearshore sea conditions for structural design and flood risk analysis. Coast Eng 88:15–26. https://doi.org/10.1016/j.coastaleng.2014.01.012

Grant WD, Madsen OS (1986) The continental shelf bottom boundary layer. Annu Rev Fluid Mech 18:265–305

Gregory JM, Griffies SM, Hughes CW, Lowe JA, Church JA, Fukimori I, Gomez N, Kopp RE, Landerer F, Cozannet GL, Ponte RM, Stammer D, Tamisiea ME, van de Wal RSW (2019) Concepts and terminology for sea level: mean, variability and change, both local and global. Surv Geophys. https://doi.org/10.1007/s10712-019-09525-z

Guérin T, Bertin X, Coulombier T, de Bakker A (2018) Impacts of wave-induced circulation in the surf zone on wave setup. Ocean Model 123:86–97. https://doi.org/10.1016/j.ocemod.2018.01.006

Guimaraes PV, Ardhuin F, Sutherland P, Accensi M, Hamon M, Pérignon Y, Thomson J, Benetazzo A, Ferrant P (2018) A Surface KInematics Buoy (SKIB) for wave-current interactions studies. Ocean Sci Discuss. https://doi.org/10.5194/os-2018-45

Gulev SK, Grigorieva V (2004) Last century changes in ocean wind wave height from global visual wave data. Geophys Res Lett. https://doi.org/10.1029/2004GL021040

Gulev SK, Grigorieva V (2006) Variability of the winter wind waves and swell in the North Atlantic and North Pacific as revealed by the voluntary observing ship data. J Clim 19:5667–5685. https://doi.org/10.1175/JCLI3936.1

Gulev SK, Grigorieva V, Sterl A, Woolf D (2003) Assessment of the reliability of wave observations from voluntary observing ships: insights from the validation of a global wind wave climatology based on voluntary observing ship data. J Geophys Res 108(C7):3236

Guza RT, Feddersen F (2012) Effect of wave frequency and directional spread on shoreline runup. Geophys Res Lett 39:L11607

Guza RT, Thornton EB (1981) Wave set-up on a natural beach. J Geophys Res 86(C5):4133–4137

Guza RT, Thornton EB (1982) Swash oscillations on a natural beach. J Geophys Res 87:483–491. https://doi.org/10.1029/JC087iC01p00483

Hanslow DJ, Nielsen P (1992) Wave setup on beaches and in river entrances. In: Proceedings of 23rd international conference on coastal Engineering, pp 240–252

Hasselmann K (1962) On the non-linear energy transfer in a gravity-wave spectrum part 1. General theory. J Fluid Mech 12(04):481–500. https://doi.org/10.1017/S0022112062000373

Hasselmann K, Chapron B, Aouf L, Ardhuin F, Collard F, Engen G, Hasselmann S, Heimbach P, Janssen P, Johnsen H, Krogstad H, Lehner S, Li J-G, Li X-M, Rosenthal W, Schulz-Stellenfleth J (2012) The ERS SAR wave mode: a breakthrough in global ocean wave observations. ERS Missions: 20 Years of Observing Earth. European Space Agency, Noordwijk, pp 165–198

Hauser D, Tison C, Amiot T, Delaye L, Corcoral N, Castillan P (2017) SWIM: the first spaceborne wave scatterometer. IEEE Trans Geosci Remote Sens 55:3000–3014. https://doi.org/10.1109/TGRS2017.2658672

Hedges T, Mase H (2004) Modified Hunt's equation incorporating wave setup. J Waterw Port Coast Ocean Eng 130:109–113

Hemer MA, Church JA, Hunter JR (2010) Variability and trends in the directional wave climate of the Southern Hemisphere. Int J Climatol 30:475–491. https://doi.org/10.1002/joc.1900

Hemer MA, Fan Y, Mori N, Semedo A, Wang XL (2013a) Projected changes in wave climate from a multi-model ensemble. Nat Clim Change 3:471–476. https://doi.org/10.1038/nclimate1791

Hemer MA, Katzfey J, Trenham CE (2013b) Global dynamical projections of surface ocean wave climate for a future high greenhouse gas emission scenario. Ocean Modell Ocean Surf Waves 70:221–245. https://doi.org/10.1016/j.ocemod.2012.09.008

Hemer MA, Wang XL, Webb A, COWCLIP contributors (2018) Report of the 2018 meeting for the WCRP-JCOMM coordinated ocean wave climate project, Paris, 21–23 May, 2018. JCOMM technical report 92. https://www.jcomm.info/index.php?option=com_oe&task=viewDocumentRecord&docID=22378

Herbers THC, Burton MC (1997) Nonlinear shoaling of directionally spread waves on a beach. J Geophys Res 102(C9):21101–21114

Herbers THC, Lentz SJ (2010) Observing directional properties of ocean swell with an acoustic doppler current profiler (ADCP). J Atmos Ocean Technol 27:210–225

Herbers THC, Janssen TT, Colbert DB, MacMahan JH (2012) Observing ocean surface waves with gps-tracked buoys. J Atmos Ocean Technol 29:944–959

Hoeke RK, McInnes KL, Kruger JC, McNaught RJ, Hunter JR, Smithers SG (2013) Widespread inundation of Pacific islands triggered by distant-source wind-waves. Glob Planet Change 108:128–138. https://doi.org/10.1016/j.gloplacha.2013.06.006

Hoeke RK, McInnes KL, O'Grady JG (2015) Wind and wave setup contributions to extreme sea levels at a tropical high island: a stochastic cyclone simulation study for Apia. Samoa J Mar Sci Eng 3:1117–1135

Holman RA (1986) Extreme value statistics for wave run-up on a natural beach. Coast Eng 9:527–544

Holman R, Haller MC (2013) Remote sensing of the nearshore. Ann Rev Mar Sci 5:95–113. https://doi.org/10.1146/annurev-marine-121211-172408

Holman RA, Sallenger AH Jr (1985) Setup and Swash on a natural beach. J Geophys Res 90(C1):945–953

Holman RA, Stanley J (2007) The history and technical capabilities of Argus. Coast Eng 54:477–491. https://doi.org/10.1016/j.coastaleng.2007.01.003

Holman R, Plant NG, Holland KT (2013) cBathy: a robust algorithm for estimating nearshore bathymetry. J Geophys Res C Oceans 118:2595–2609. https://doi.org/10.1002/jgrc.20199

Holthuijsen LH, Herman A, Booij N (2003) Phase-decoupled refraction-diffraction for spectral wave models. Coast Eng 49:91–305

Hunt IA (1959) Design of seawalls and breakwaters. J Waterw Harbors Div 85:123–152

Idier D, Bertin X, Thompson P, Pickering MD (2019) Interactions between mean sea level, tide, surge, waves and flooding: mechanisms and contributions to sea level variations at the coast. Surv Geophys. https://doi.org/10.1007/s10712-019-09549-5

Inch K, Davidson M, Masselink G, Russell P (2017) Observations of nearshore infragravity wave dynamics under high energy swell and wind-wave conditions. Cont Shelf Res 138:19–31. https://doi.org/10.1016/j.csr.2017.02.010

Iribarren CR, Nogales C (1949) Protection des ports. In: XVIIth international navigation congress. Lisbon, Portugal, pp 31–80

Izaguirre C, Méndez FJ, Menéndez M, Losada IJ (2011) Global extreme wave height variability based on satellite data. Geophys Res Lett. https://doi.org/10.1029/2011GL047302

Jackson FC, Walton WT, Baker PL (1985) Aircraft and satellite measurement of ocean wave directional spectra using scanning-beam microwave radars. J Geophys Res 90:987–1004

Janssen TT, Herbers THC, Battjes JA (2006) Generalized evolution equation for nonlinear surface gravity waves over two-dimensional topography. J Fluid Mech 552:393–418

Jensen RE, Swail VR, Bouchard RH, Riley RE, Hesser TJ, Blaseckie M, MacIsaac C (2015) Field laboratory for ocean sea state investigation and experimentation: FLOSSIE intra-measurement evaluation of 6 N wave buoy systems. In: Proceedings of the 114th international workshop on wave hindcasting and forecasting & 5th coastal hazard symposium

Ji C, Zhang Q, Wu Y (2018) An empirical formula for maximum wave setup based on a coupled wave-current model. Ocean Eng 147:215–226

Jia G, Taflanidis AA (2013) Kriging metamodeling for approximation of high-dimensional wave and surge responses in real-time storm/hurricane risk assessment. Comput Methods Appl Mech Eng 261:24–38

Karunarathna H, Caraballo JH, Kuriyama Y, Mase H, Ranasinghe R, Reeve DE (2016) Linkages between sediment composition, wave climate and beach profile variability at multiple timescales. Mar Geol 381:194–208

Kennedy A, Westerink J, Smith J, Hope M, Hartman M, Taflanidis A, Tanaka S, Westerink H, Cheung K, Smith T, Hamann M, Minamide M, Ota A, Dawson C (2012) Tropical cyclone inundation potential on the hawaiian islands of Oahu and Kauai. Ocean Model 52–53:54–68

Kerbaol V, Chapron B, Vachon P (1998) Analysis of ERS-1/2 synthetic aperture radar wave mode imagettes. J Geophys Res 103(C4):7833–7846

Kim SY, Yasuda T, Mase H (2008) Numerical analysis of effects of tidal variations on storm surges and waves. App Ocean Res 30(4):311–322. https://doi.org/10.1016/j.apor.2009.02.003

Komar P (1998) Beach processes and sedimentation, 2nd edn. Prentice Hall, New Jersey

Kudryavtsev V, Yurovskaya M, Chapron B, Collard F, Donlon C (2017) Sun glitter imagery of surface waves. Part 2: waves transformation on ocean currents. J Geophys Res. https://doi.org/10.1002/2016jc012426

Kumar N, Voulgaris G, Warner JC, Olabarrieta M (2012) Implementation of the vortex force formalism in the coupled ocean-atmosphere-wavesediment transport (COAWST) modeling system for inner shelf and surf zone applications. Ocean Model 47:65–95. https://doi.org/10.1016/j.ocemod.2012.01.003

Laugel A, Menendez M, Benoit M, Mattarolo G, Méndez F (2014) Wave climate projections along the French coastline: dynamical versus statistical downscaling methods. Ocean Model 84:35–50. https://doi.org/10.1016/j.ocemod.2014.09.002

Longuet-Higgins M, Stewart R (1962) Radiation stress and mass transport in gravity waves, with application to surf beats. J Fluid Mech 13(4):481–504

Longuet-Higgins MS, Stewart R (1964) Radiation stresses in water waves; a physical discussion, with applications. Deep Sea Res Oceanogr Abstracts 11:529–562

Longuet-Higgins MS, Cartwright DE, Smith ND (1963) Observations of the directional spectrum of sea waves using the motions of a floating buoy. In: Ocean wave spectra, proceedings of a conference, Easton, Maryland, pp 111–136, National Academy of Sciences, Prentice-Hall

Luijendijk A, Hagenaars G, Ranasinghe R, Baart F, Donchyts G, Aarninkhof S (2018) The state of the world's beaches. Sci Rep 8:6641

Lumpkin T, Ozgokmen T, Centurioni L (2016) Advances in the application of surface drifters. Ann Rev Mar Sci. https://doi.org/10.1146/annurev-marine-010816-060641

Magne R, Belibassakis K, Herbers THC, Ardhuin F, O'Reilly WC, Rey V (2007) Evolution of surface gravity waves over a submarine canyon. J Geophys Res 112:C01002. https://doi.org/10.1029/2005JC003035

Malhadas MS, Leitão PC, Silva A, Neves R (2009) Effect of coastal waves on sea-level in Óbidos Lagoon, Portugal. Cont Shelf Res 29(9):1240–1250

Marchesiello P, Benshila R, Almar R, Uchiyama Y, McWilliams JC, Shchepetkin A (2015) On tridimensional rip current modeling. Ocean Model 96:36–48. https://doi.org/10.1016/j.ocemod.2015.07.003

Martins K, Blenkinsopp CE, Power HE, Bruder B, Puleo JA, Bergsma EWJ (2017) High-resolution monitoring of wave transformation in the surf zone using a LiDAR scanner array. Coast Eng 128:37–43. https://doi.org/10.1016/j.coastaleng.2017.07.007

Martins K, Blenkinsopp CE, Deigaard R, Power HE (2018) Energy dissipation in the inner surf zone: new insights from LiDAR-based roller geometry measurements. J Geophys Res Oceans (in press)

Mase H (1989) Random wave runup height on gentle slope. J Waterw Port Coast Ocean Eng 115:649–661

Masselink G, Russell P, Turner I, Blenkinsopp C (2009) Net sediment transport and morphological change in the swash zone of a high-energy sandy beach from swash event to tidal cycle time scales. Mar Geol 267:18–35. https://doi.org/10.1016/j.margeo.2009.09.003

Masselink G, Castelle B, Scott T, Dodet G, Suanez S, Jackson D, Floc'h F (2016) Extreme wave activity during 2013/2014 winter and morphological impacts along the Atlantic coast of Europe. Geophys Res Lett 43:2135–2143. https://doi.org/10.1002/2015GL067492

Mastenbroek C, Burgers G, Janssen PAEM (1993) The dynamical coupling of a wave model and a storm surge model through the atmospheric boundary layer. J Phys Oceanogr 23:1856–1866

Matsuba Y, Sato S (2018) Nearshore bathymetry estimation using UAV. Coast Eng J 60:51–59. https://doi.org/10.1080/21664250.2018.1436239

McWilliams JC, Restrepo JM, Lane EM (2004) An asymptotic theory for the interaction of waves and currents in coastal waters. J Fluid Mech 511:135–178

Melet A, Almar R, Meyssignac B (2016) What dominates sea level at the coast: a case study for the Gulf of Guinea. Ocean Dyn 66:623–636

Melet A, Meyssignac B, Almar R, Le Cozannet G (2018) Under-estimated wave contribution to sea-level rise. Nat Clim Change 8:234–239

Melet A, Meyssignac B, Almar R, Le Cozannet G (2019) Reply to ''Waves do not contribute to global sea-level rise''. Nat Clim Change 9:3. https://doi.org/10.1038/s41558-018-0378-4

Menéndez M, Méndez FJ, Losada IJ, Graham NE (2008) Variability of extreme wave heights in the northeast Pacific Ocean based on buoy measurements. Geophys Res Lett. https://doi.org/10.1029/2008GL035394

Mentaschi L, Vousdoukas MI, Voukouvalas E, Dosio A, Feyen L (2017) Global changes of extreme coastal wave energy fluxes triggered by intensified teleconnection patterns. Geophys Res Lett 44:2416–2426. https://doi.org/10.1002/2016GL072488

Merrifield MA, Becker JM, Ford M, Yao Y (2014) Observations and estimates of wave-driven water level extremes at the Marshall Islands. Geophys Res Lett 41:7245–7253. https://doi.org/10.1002/2014GL061005

Morim J, Hemer M, Cartwright N, Strauss D, Andutta F (2018) On the concordance of 21st century wind-wave climate projections. Glob Planet Change 167:160–171. https://doi.org/10.1016/j.glopl acha.2018.05.005

Moura T, Baldock TE (2017) Remote sensing of the correlation between breakpoint oscillations and infra-gravity waves in the surf and swash zone. J Geophys Res Oceans 122(4):3106–3122

Munk WH, Traylor MA (1947) Refraction of ocean waves: a process linking underwater topography to beach erosion. J Geol LV:1–26

Munk WH, Miller GR, Snodgrass FE, Barber NF (1963) Directional recording of swell from distant storms. Phil Trans R Soc Lond Ser A Math Phys Eng Sci 255:505–584. https://doi.org/10.1098/rsta.1963.0011

Neumann B, Vafeidis AT, Zimmermann J, Nicholls RJ (2015) Future coastal population growth and exposure to sea-level rise and coastal flooding—a global assessment. PLoS ONE. https://doi.org/10.1371/journal.pone.0118571

Nicolae-Lerma A, Pedreros R, Senechal N (2016) Wave set-up and run-up variability on a complex barred beach during highly dissipative storm conditions. J Coast Res 75:882–886. https://doi.org/10.2112/SI75-177.1

Nicolae-Lerma A, Pedreros R, Robinet A, Sénéchal N (2017) Simulating wave setup and runup during storm conditions on a complex barred beach. Coast Eng 123:29–41

Nielsen P, DJ Hanslow (1991) Wave runup distributions on natural beaches. J Coast Res 1139–1152

Nouguier F, Chapron B, Collard F, Mouche A, Rascle N, Ardhuin F, Wu X (2018) Sea surface kinematics from near-nadir radar measurements. IEEE Trans Geosci Remote Sens. https://doi.org/10.1109/tgrs2018.2833200

O'Reilly WC, Guza RT (1993) A comparison of two spectral wave models in the Southern California Bight. Coast Eng 19:263–282

Overeem I, Anderson RS, Wobus CW, Clow GD, Urban FE, Matell N (2011) Sea ice loss enhances wave action at the Arctic coast. Geophys Res Lett. https://doi.org/10.1029/2011GL048681

Ozer J, Padilla-Hernandez R, Monbaliub J, Fanjul EA, Albiach JCC, Osuna P, Yu JC, Wolf J (2000) A coupling module for tides, surges and waves. Coast Eng 41(1–3):95–124

Passarella M, Goldstein EB, De Muro S, Coco G (2018) The use of genetic programming to develop a predictor of swash excursion on sandy beaches. Nat Hazards Earth Syst Sci 18:599–611. https://doi.org/10.5194/nhess-18-599-2018

Passaro M, Fenoglio-Marc L, Cipollini P (2015) Validation of significant wave height from improved satellite altimetry in the German Bight. IEEE Trans Geosci Remote Sens 53:2146–2156

Pearson J, Bruce T, Allsop N (2001) Prediction of wave overtopping at steep seawalls—variabilities and uncertainties. Proc Waves 1:1797–1808

Pedreros R, Idier D, Muller H, Lecacheux S, Paris F, Yates-Michelin M, Dumas F, Pineau-Guillou L, Sénéchal N (2018) Relative contribution of wave setup to the storm surge: observations and modeling based analysis in open and protected environments (Truc Vert beach and Tubuai island). In: Shim J-S, Chun I, Lim HS (eds) Proceedings from the international coastal symposium (ICS) 2018 (Busan, Republic of Korea). J Coast Res 85:1046–1050. Coconut Creek (Florida), ISSN 0749-0208

Perez J, Menendez M, Camus P, Mendez FJ, Losada IJ (2015) Statistical multi-model climate projections of surface ocean waves in Europe. Ocean Model 96:161–170. https://doi.org/10.1016/j.ocemod.2015.06.001

Pianca C, Holman R, Siegle E (2015) Shoreline variability from days to decades: results of long-term video imaging. J Geophys Res Oceans 120(3):2159–2178

Poate TG, McCall RT, Masselink G (2016) A new parameterisation for runup on gravel beaches. Coast Eng 117:176–190. https://doi.org/10.1016/j.coastaleng.2016.08.003

Pomeroy A, Lowe R, Symonds G, Van Dongeren A, Moore C (2012) The dynamics of infragravity wave transformation over a fringing reef. J Geophys Res. https://doi.org/10.1029/2012jc008310

Poupardin A, Idier D, de Michele M, Raucoules D (2016) Water depth inversion from a single SPOT-5 dataset. IEEE Trans Geosci Remote Sens 54:2329–2342. https://doi.org/10.1109/TGRS2015.2499379

Powell KA (1990) Predicting short term profile response for shingle beaches. Hydraulics Research Limited, Wallingford, Oxfordshire. Report SR2 19

Power HE, Gharabaghi B, Bonakdari H, Robertson B, Atkinson AL, Baldock TE (2019) Prediction of wave runup on beaches using Gene-Expression Programming and empirical relationships. Coast Eng 144:47–61

Pullen T, Allsop N, Bruce T, Kortenhaus A, Schüttrumpf H, Van der Meer J (2007) EurOtop wave overtopping of sea defences and related structures: assessment manual. Environ Agency, UK

Purkis SJ (2018) Remote sensing tropical coral reefs: the view from above. Ann Rev Mar Sci 10(1):149–168. https://doi.org/10.1146/annurev-marine-121916-063249

Quilfen Y, Yurovskaya M, Chapron B, Ardhuin F (2018) Storm waves sharpening in the Agulhas current: satellite observations and modeling. Remote Sens Environ 216:561–571. https://doi.org/10.1016/j.rse.2018.07.020

Ranasinghe R (2016) Assessing climate change impacts on open sandy coasts: a review. Earth-Sci Rev 160:320–332. https://doi.org/10.1016/j.earscirev.2016.07.011

Raubenheimer B, Guza R, Elgar S (2001) Field observations of wave-driven setdown and setup. J Geophys Res Oceans 106(C3):4629–4638

Raucoules D, de Michele M, Idier D, Smai F, Foumelis M, Boulahya F, Volden E, Drakopoulou V, Przemysław M (2019) BATHYSENT—a method to retrieve coastal bathymetry from sentinel-2). In: IEEE international geoscience and remote sensing symposium (IGARSS)

Rawat A, Ardhuin F, Ballu V, Crawford W, Corela C, Aucan J (2014) Infragravity waves across the oceans. Geophys Res Lett 41(22):7957–7963. https://doi.org/10.1002/2014GL061604

Rhein M et al (2013) Observations: ocean. In: Stocker TF, Qin D, Plattner G-K, Tignor M, Allen SK, Boschung J, Nauels A, Xia Y, Bex V, Midgley PM (eds) Climate change 2013: the physical science basis. contribution of working group I to the fifth assessment report of the intergovernmental panel on climate change. Cambridge University Press, Cambridge, pp 255–316. https://doi.org/10.1017/cbo9781107415324.010

Roberts TM, Wang P, Kraus NC (2010) Limits of wave runup and corresponding beach-profile change from large-scale laboratory data. J Coast Res 26:184–198

Roelvink D, Reniers A, van Dongeren A, van Thiel de Vries J, McCall R, Lescinski J (2009) Modelling storm impacts on beaches, dunes and barrier islands. Coast Eng 56:1133–1152. https://doi.org/10.1016/j.coastaleng.2009.08.006

Roelvink D, McCall R, Mehvar S, Nederhoff K, Dastgheib A (2018) Improving predictions of swash dynamics in XBeach: the role of groupiness and incident-band runup. Coast Eng 134:103–123. https://doi.org/10.1016/j.coastaleng.2017.07.004

Rohmer J, Idier D (2012) A meta-modelling strategy to identify the critical offshore conditions for coastal flooding. Nat Hazards Earth Syst Sci 12:2943–2955. https://doi.org/10.5194/nhess-12-2943-2012

Rohmer J, Lecacheux S, Pedreros R et al (2016) Dynamic parameter sensitivity in numerical modelling of cyclone-induced waves: a multi-look approach using advanced meta-modelling techniques. Nat Hazards 84:1765. https://doi.org/10.1007/s11069-016-2513-8

Roland A, Ardhuin F (2014) On the developments of spectral wave models: numerics and parameterizations for the coastal ocean. Ocean Dyn 64(6):833–846. https://doi.org/10.1007/s10236-014-0711-z

Romano A, Bellotti G, Briganti R, Franco L (2015) Uncertainties in the physical modelling of the wave overtopping over a rubble mound breakwater: the role of the seeding number and of the test duration. Coast Eng 103:15–21. https://doi.org/10.1016/j.coastaleng.2015.05.005

Romeiser R, Graber HC (2018) Advanced ocean wave retrieval from time series of spotlight SAR subaperture images, EUSAR 2018. In: 12th European conference on synthetic aperture radar

Rueda A, Gouldby B, Méndez F, Tomás A, Losada I, Lara J, Díaz-Simal P (2016) Coastal flood risk assessment. J Flood Risk Manag 9:390–401. https://doi.org/10.1111/jfr3.12204

Rueda A, Vitousek S, Camus P, Tomas A, Epejo A, Losada IJ, Barnard P, Erikson L, Ruggiero P, Reguero BG, Mendez FJ (2017) A global classification of coastal flood hazard climates associated with large-scale oceanographic forcing. Sci Rep 7:5038

Ruessink BG (2010) Observations of turbulence within a natural surf zone. J Phys Oceanogr 40:2696–2712. https://doi.org/10.1175/2010JPO4466.1

Ruessink BG, Kleinhans MG, van den Beukel PGL (1998) Observations of swash under highly dissipative conditions. J Geophys Res 103:3111–3118. https://doi.org/10.1029/97JC02791

Ruggiero P, Komar PD, Marra JJ, McDougal WG, Beach RA (2001) Wave runup, extreme water levels and the erosion of properties backing beaches. J Coastal Res 17:407–419

Ruggiero P, Holman R, Beach R (2004) Wave run-up on a high-energy dissipative beach. J Geophys Res C Oceans 109(6):C06025, 1–12. https://doi.org/10.1029/2003jc002160

Ruggiero P, Komar PD, Allan JC (2010) Increasing wave heights and extreme value projections: the wave climate of the U.S. Pacific Northwest. Coast Eng 57:539–552. https://doi.org/10.1016/j.coastaleng.2009.12.005

Rusu L, Bernardino M, Guedes Soares C (2011) Modelling the influence of currents on wave propagation at the entrance of the Tagus estuary. Ocean Eng 38(10):1174–1183. https://doi.org/10.1016/j.oceaneng.2011.05.016

Saville T (1961) Experimental determination of wave set-up. In: Proceedings of the second technical conference on hurricanes, US Dept. of Commerce, National Hurricane Res. Proj, 1961, pp 242–252

Semedo A, Sušelj K, Rutgersson A, Sterl A (2010) A global view on the wind sea and swell climate and variability from ERA-40. J Clim 24:1461–1479. https://doi.org/10.1175/2010JCLI3718.1

Send U, Weller RA, Wallace D, Chavez F, Lampitt R, Dickey T, Honda M, Nittis K, Lukas R, McPhaden M, Feely R (2010) OceanSITES. In: Hall J, Harrison DE, Stammer D (eds) Proceedings of Ocean-Obs'09: sustained ocean observations and information for society, Vol. 2. European Space Agency, pp 913–922

Senechal N, Coco G, Bryan KR, Holman RA (2011) Wave runup during extreme storm conditions. J Geophys Res 116:C07032. https://doi.org/10.1029/2010JC006819

Seneviratne SI et al (2012) Changes in climate extremes and their impacts on the natural physical environment. In: Field CB, Barros V, Stocker TF, Dahe Q (eds) Managing the risks of extreme events and disasters to advance climate change adaptation. Cambridge University Press, Cambridge, pp 109–230. https://doi.org/10.1017/cbo9781139177245.006

Sepulveda HH, Queffeulou P, Ardhuin F (2015) Assessment of SARAL AltiKa wave height measurements relative to buoy, Jason-2 and Cryosat-2 data. Mar Geodesy 38(S1):449–465. https://doi.org/10.1080/01490419.2014.1000470

Serafin KA, Ruggiero P, Stockdon HF (2017) The relative contribution of waves, tides, and nontidal residuals to extreme total water levels on US West Coast sandy beaches. Geophys Res Lett 44:1839–1847

Sheremet A, Staples T, Ardhuin F, Suanez S, Fichaut B (2014) Observations of large infragravity-wave run-up at Banneg island, France. Geophys Res Lett. https://doi.org/10.1002/2013gl058880

Smit PB, Janssen TT, Herbers THC, Taira T, Romanowicz BA (2018) Infragravity wave radiation across the shelf break. J Geophys Res Oceans 123:4483–4490. https://doi.org/10.1029/2018JC013986

Smith JA (2006) Wave-current interactions in finite-depth. J Phys Oceanogr 36:1403–1419

Stewart AL, Ferrari R, Thompson AF (2013) On the importance of surface forcing in conceptual models of the deep ocean. J Phys Oceanogr 44:891–899. https://doi.org/10.1175/JPO-D-13-0206.1

Stockdon HF, Holman RA, Howd PA, Sallenger AH Jr (2006) Empirical parameterization of setup, swash, and runup. Coast Eng 53:573–588. https://doi.org/10.1016/j.coastaleng.2005.12.005

Stockdon HF, Thompson DM, Plant NG, Long JW (2014) Evaluation of wave runup predictions from numerical and parametric models. Coast Eng 92:1–11

Stopa JE, Ardhuin F, Girard-Ardhuin F (2016) Wave climate in the Arctic 1992-2014: seasonality and trends. Cryosphere 10:1605–1629. https://doi.org/10.5194/tc-10-1605-2016

Stopa JE, Ardhuin F, Stutzmann E, Lecocq T (2019) Sea state trends and variability: consistency between models, altimeters, buoys, and seismic data (1979–2016). J Geophys Res Oceans. https://doi.org/10.1029/2018JC014607

Suanez S, Cancouët R, Floc'h F, Blaise E, Ardhuin F, Filipot J.-F, Cariolet J.-M, Delacourt C (2015) Observations and predictions of wave runup, extreme water levels, and medium-term dune erosion during storm conditions. J Mar Sci Eng 3:674–698. https://doi.org/10.3390/jmse3030674

Suzuki N, Fox-Kemper B (2016) Understanding Stokes forces in the wave-averaged equations. J Geophys Res Oceans 121:3579–3596. https://doi.org/10.1002/2015JC011566

Symonds G, Huntley DA, Bowen AJ (1982) Two-dimensional surf beat: long wave generation by a time-varying breakpoint. J Geophys Res Oceans 87:492–498. https://doi.org/10.1029/JC087iC01p00492

The WAVEWATCH III R Development Group (2016) User manual and system documentation of WAVE-WATCH III R version 5.16," Tech. Note 329, NOAA/NWS/NCEP/MMAB, College Park, MD, USA, 2016. 326 pp. + Appendices

Thomson J (2012) Wave breaking dissipation observed with "swift" drifters. J Atmos Ocean Technol 29:1866–1882. https://doi.org/10.1175/JTECH-D-12-00018.1

Thompson RORY, Hamon BV (1980) Wave setup of harbor water levels. J Geophys Res Oceans 85:1151–1152. https://doi.org/10.1029/JC085iC02p01151

Thornton EB, Guza RT (1983) Transformation of wave height distribution. J Geophys Res Oceans 88:5925–5938. https://doi.org/10.1029/JC088iC10p05925

Torres-Freyermuth A, Puleo JA, Pokrajac D (2013) Modeling swash-zone hydrodynamics and shear stresses on planar slopes using reynolds-averaged naviersstokes equations. J Geophys Res 118:1019–1033. https://doi.org/10.1002/jgrc.20074

Tuah H, Hudspeth RT (1982) Comparisons of numerical random sea simulations. J Waterw Port Coast Ocean Div ASCE 108(4):569–584

Turner IL, Harley MD, Drummond CD (2016) UAVs for coastal surveying. Coast Eng 114:19–24. https://doi.org/10.1016/j.coastaleng.2016.03.011

Van der Meer JW, Stam C-JM (1992) Wave runup on smooth and rock slopes of coastal structures. J Waterw Port Coast Ocean Eng 118:534–550. https://doi.org/10.1061/(ASCE)0733-950X(1992)118:5(534)

Vitousek S, Barnard PL, Fletcher CH, Frazer N, Erikson L, Storlazzi CD (2017) Doubling of coastal flooding frequency within decades due to sea-level rise. Nature 7:1399

Vousdoukas MI, Velegrakis AF, Dimou K, Zervakis V, Conley DC (2009) Wave run-up observations in microtidal, sediment-starved pocket beaches of the Eastern Mediterranean. J Mar Syst 78:S37–S47

Vousdoukas MI, Wziatek D, Almeida LP (2012) Coastal vulnerability assessment based on video wave run-up observations at a mesotidal, steep-sloped beach. Ocean Dyn 62(1):123–137

Vousdoukas MI et al (2016) Developments in large-scale coastal flood hazard mapping. Nat Hazards Earth Syst Sci 16:1841–1853

Vousdoukas MI, Mentaschi L, Voukouvalas E, Verlaan M, Feyen L (2017) Extreme sea levels on the rise along Europe's coasts. Earth's Future 5:304–323

Vousdoukas MI, Mentaschi L, Voukouvalas E, Verlaan M, Jevrejeva S, Jackson LP, Feyen L (2018a) Global probabilistic projections of extreme sea levels show intensification of coastal flood hazard. Nat Commun 9:2360

Vousdoukas MI, Mentaschi L, Voukouvalas E, Bianchi A, Dottori F, Feyen L (2018b) Climatic and socio-economic controls of future coastal flood risk in Europe. Nat Clim Change 8:776–780

Walstra DJR, Roelvink J, Groeneweg J (2000) Calculation of wave-driven currents in a 3D mean flow model. In: Proceedings of the 27th international conference on coastal engineering, Sydney, vol 2, pp 1050–1063, ASCE, 2000

Wandres M, Pattiaratchi C, Hemer MA (2017) Projected changes of the southwest Australian wave climate under two atmospheric greenhouse gas concentration pathways. Ocean Model 117:70–87

Wang XL, Swail VR (2001) Changes in extreme wave heights in Northern Hemisphere oceans and related atmospheric circulation regimes. J Clim 14:2204–2221. https://doi.org/10.1175/1520-0442(2001)014,2204:COEWHI2.0.CO;2

Wang XL, Swail VR (2006) Climate change signal and uncertainty in projections of ocean wave heights. Clim Dyn 26:109–126. https://doi.org/10.1007/s00382-005-0080-x

Wang XL, Feng Y, Swail VR (2014) Changes in global ocean wave heights as projected using multimodel CMIP5 simulations. Geophys Res Lett 41:1026–1034. https://doi.org/10.1002/2013GL058650

Wassing F (1957) Model investigation on wave run-up carried out in the Netherlands during the past twenty years. In: Proccedings of the 6th international coastal engineering conference, American Society of Civil Engineers, pp 700–714

Wenneker I, Spelt B, Peters H, de Ronde J (2016) Overview of 20 years of field measurements in the coastal zone and at the Petten sea dike in the Netherlands. Coast Eng 109:96–113. https://doi.org/10.1016/j.coastaleng.2015.12.009

Williams HE, Briganti R, Pullen T (2014) The role of offshore boundary conditions in the uncertainty of numerical prediction of wave overtopping using non-linear shallow water equations. Coas En 89:30–44. https://doi.org/10.1016/j.coastaleng.2014.03.003

WISE Group (2007) Wave modelling—the state of the art. Prog Oceanogr 75:603–674. https://doi.org/10.1016/j.pocean.2007.05.005

Woodworth PL, Melet A, Marcos M, Ray RD, Wöppelmann G, Sasaki YN, Cirano M, Hibbert A, Huthnance JM, Monserrat S, Merrifield MA (2019) Forcing factors affecting sea level changes at the coast. Surv Geophys. https://doi.org/10.1007/s10712-019-09531-1

Wong PP et al. In: Climate change 2014: impacts, adaptation, and vulnerability. Field CB et al (eds). IPCC, Cambridge Univ. Press, pp 361–409

Wright LD, Short AD (1984) Morphodynamic variability of surf zones and beaches: a synthesis. Mar Geol 56:93–118

Young IR, Ribal A (2019) Multiplatform evaluation of global trends in wind speed and wave height. Science 364:548. https://doi.org/10.1126/science.aav9527

Young IR, Zieger S, Babanin AV (2011) Global trends in wind speed and wave height. Science 332:451–455. https://doi.org/10.1126/science.1197219

Zhang WZ, Shi F, Hong HS, Shang SP, Kirby JT (2010) Tide-surge Interaction Intensified by the Taiwan Strait. J Geophys Res 115:C06012. https://doi.org/10.1029/2009JC005762

Zijlema M, Stelling G, Smit P (2011) Swash: an operational public domain code for simulating wave fields and rapidly varied flows in coastal waters. Coast Eng 58:992–1012. https://doi.org/10.1016/j.coastaleng.2011.05.015